01 Mar 1968

Deformation and energy absorption capacity of steel structures in the inelastic range

Theodore V. Galambos

BULLETIN No. 8, MARCH, 1968 — *Galambos* — DEFORMATION AND ENERGY ABSORPTION CAPACITY OF STEEL STRUCTURES IN THE INELASTIC RANGE

STEEL RESEARCH for construction

DEFORMATION AND ENERGY ABSORPTION CAPACITY OF STEEL STRUCTURES IN THE INELASTIC RANGE

—Theodore V. Galambos

Committee of Structural Steel Producers • Committee of Steel Plate Producers

american iron and steel institute

150 East 42nd Street, New York, N.Y. 10017

BULLETIN No. 8, MARCH, 1968

SUMMARY REPORT

on

DEFORMATION AND ENERGY ABSORPTION CAPACITY OF STEEL STRUCTURES IN THE INELASTIC RANGE

to

AMERICAN IRON AND STEEL INSTITUTE

March 1967

by

Theodore V. Galambos

Civil and Environmental Engineering Department

Sever Institute of Technology

Washington University

St. Louis, Missouri

Printed in U.S.A. 3/68 3500

ABSTRACT

This report summarizes the status of knowledge on the inelastic deformability of steel members and frames. It demonstrates that the inelastic response of planar beams, beam-columns, connections and frames is well understood and can be adequately, though conservatively, predicted by theory provided the loading is static, proportional and monotonic, and adequate provisions are made to inhibit premature local and lateral-torsional instability. The report reviews the available theoretical work, and examines the experimental evidence. It shows that the inelastic rotation capacity, which defines also the "ductility factor" and the inelastic energy absorption capacity, is both predictable and large enough to meet the requirements of plastically designed frames.

The report demonstrates that the knowledge of the behavior of members and frames subjected to non-proportional or reversible loading, which may be the result of dynamic phenomena, is not complete. Methods of frame analysis are available, but information needs to be generated on the inelastic behavior of individual structural components under reversed loading. This information is vital for the performance of a proper dynamic analysis. A similar need exists in the area of biaxially loaded structures.

The report considers separately the available research on beams, beam-columns, connections and frames. Particular emphasis is placed on the inelastic deformability. Each section of the report contains specific suggestions for further research and study. Selected references appear at the end of the report.

The large amount of research performed for the development of plastic design has relevance for the study of the behavior of structures subjected to earthquake motion or blast, because it provides information on basic behavior, and it defines methods of analysis and experimentation. This research does not, however, give all the answers, and some additional areas need to be investigated.

ACKNOWLEDGEMENTS

This literature survey was made possible by a grant from the Committees of Structural Steel and Steel Plate Producers of American Iron and Steel Institute. The encouragement and assistance of Dr. I. M. Viest is gratefully acknowledged. Mr. Paul Heaton assisted in some phases of this work. The report was typed by Mrs. Lois Simons.

Table of Contents

I. INTRODUCTION

Structural engineers are becoming increasingly interested in using the maximum strength of a structure (or its "ultimate" strength or "collapse" strength) as one criterion of design. This interest is due to a variety of complex reasons, one of which is the more economical use of structural materials than in a design based on purely elastic behavior. It is also realized that the use of the elastic limit as a design criterion can not always account for instability effects in a rational manner. In some design situations, particularly when resistance to earthquake motions and blast shocks is involved, it is necessary to count on the energy absorbed by inelastic deformations.

"Maximum strength" design, better known as "plastic" design, depends on the ability of the structure to deform into the inelastic range without fracture or the loss of its capacity to resist forces as the deformations increase. The structure and its components must be "ductile."

A vast amount of research has been performed on a multitude of problems related to inelastic behavior for both steel and concrete structures. The present study is restricted to a survey of research on steel-framed structures and components. Several previous studies collected, classified and evaluated the research on the inelastic behavior of framed steel structures [Refs. 1-1, 1-2, 1-3 and 1-4]. These surveys provided supporting evidence for design rules for structures under static loads [1-5].

The purpose of this report is to collect and evaluate the available information on inelastic deformability and energy absorption capacity. The emphasis is thus on "deformability" rather than on "load capacity." The reason for collecting this information is to provide structural designers with a clear picture of just how much a steel structure can deform, and to draw the attention of researchers to areas in which more work is needed. The principal impetus for this literature survey has been to suggest how the research data developed for steel structures under static loads have relevance for structures subjected to earthquake motions. This topic is discussed in the conclusion of this report.

The report evaluates both the theoretical and the experimental information on the inelastic deformability of steel beams, beam-columns, connections and frames. The list of references contains most of the recent English language papers.

Definition of Terms

Before starting a description of the inelastic behavior of individual steel components, it is well to discuss some general terminology. The solid curve in Fig. 1 shows a typical end moment-end rotation curve for a steel member or connection under monotonic deformation. Here "monotonic deformation" indicates that the member is deformed in one direction past the maximum load and into the unloading range. The member responds first in an elastic manner (OA, Fig. 1). After initiation of yielding the increments of deformation increase for equal increments of the moment until the peak moment M_M is reached. With further deformation the moment must be reduced to maintain equilibrium and finally the moment capacity is fully exhausted.

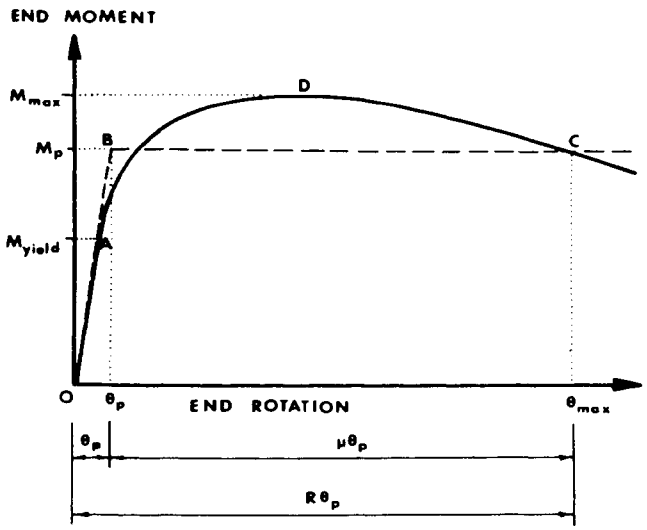

Fig. 1 Typical member moment-rotation curve.

The non-linear behavior is caused by:

(1) geometric non-linearities – i.e., the force distribution may be changed by the deflections (e.g., the "P–Δ" effect in beam-columns).
(2) material non-linearities – such as yielding and strain-hardening of the material.
(3) non-linearities due to local or lateral-torsional instability.
(4) non-linearities of the connection elements.

These non-linearities cause a continual reduction in the stiffness of the member until equilibrium can only be maintained by a reduction of the moment capacity.

In the non-linear range the relationship between the forces and deformations becomes highly complex, and it is usually convenient to represent the curve OADC by the two straight lines OAB and BC (Fig. 1). Such a representation is called the "ideal elastic-plastic relationship." It is first assumed that the member remains elastic until severe loss of stiffness takes place, and the moment thereafter is assumed to remain constant with an increasing deformation. Severe loss of stiffness usually corresponds to the full plastification of the cross section, that is, the attainment of the full plastic moment. [1-2]

The particular question to which this report is addressed is: What is the deformation θ_M at which the moment begins to drop off substantially below the maximum moment M_M? In Fig. 1, θ_M corresponds to the rotation at the intersection between the actual M–θ curve and the plastic moment level. This is an arbitrary cut-off, but it is a more realistic estimate of deformability than the rather ill-defined rotation at the maximum moment. In the later discussions each situation will require a specific definition of the final rotation, θ_M, and this will be stated.

The deformability of a member will be either determined as the absolute value of the rotation θ_M, or the "rotation capacity," which is defined as

$$R = \frac{\theta_M}{\theta_p} - 1 \qquad (1)$$

or the "ductility factor," which is defined as

$$\mu = \frac{\theta_M}{\theta_p} = R + 1 \qquad (2)$$

The related dimensionless terms R and μ are illustrated in Fig. 1. The rotation θ_p in Fig. 1 is the hypothetical elastic rotation caused by M_p. In a more general sense, θ_p in Eq. 1 and 2 represents the extent of the elastic range of deformation. In situations where it is difficult to define a meaningful value for θ_p, the final rotation θ_M is a useful measure of deformability.

2. BEAMS

Beams are here defined as members for which the axial and shear forces are so small that their effects on the over all behavior are negligible. [2-1] Such members comprise most horizontal members in multistory frames.

It appears that the available plastically designed, unbraced multistory frames developed the majority of the plastic hinges in the beams, and that inelastic action in the columns was limited. The British approach to the plastic design of tall frames is based on the deliberate exclusion of plastic hinges from the columns. [2-2] The probable reason for this is the concern for inelastic instability, particularly for lateral-torsional buckling. The largest reported steel frame designed before 1967 by plastic design is the 3-bay, 24-story frame C of the Lehigh Summer Conference notes. [2-3] In this frame only eight out of a total of 63 plastic hinges form in the columns. [2-4]

All of these frames were designed on the basis of the "weak beam, strong column" concept. However, if the stiffness of an unbraced rigid frame is increased by increasing the beam sizes, the proportion of beam-to-column hinges may become altered. It is reasonable to expect that efficiently designed earthquake-resistant structures will also depend largely on the capacity of the beams to absorb energy. [2-5] Thus for multistory frames it can be expected that most of the inelastic action will take place in the beams.

On the surface, the prediction of the inelastic behavior of beams is simple. However, this simplicity is deceptive, and when the mass of data is evaluated there still remain some unanswered questions about beams.

Most of the research on steel beams has been confined to rolled or built-up wide-flange beams of A36 and A441 steel. The following discussion is limited to such beams.

Besides the yield stress, σ_y, and the cross-sectional geometry, which define the fully plastic moment, M_p, other important structural properties of steel wide-flange beams are the *unbraced slenderness ratio* and the *width-thickness ratios of its plate elements.* Depending on the magnitudes of these ratios, the performance of beams lies in one of the three regions shown in Fig. 2. This figure shows schematically the variation of the moment capacity (upper region) and the rotation capacity (lower region) with the unbraced slenderness ratio and the width-thickness ratio. The unbraced slenderness ratio is the governing parameter of lateral-torsional instability and the width-thickness ratios control local buckling. When either of these ratios is large, the maximum moment is curtailed by elastic buckling. When these ratios are relatively small, the full plastic moment is reached or exceeded. In the intermediate or transition range buckling occurs under partially inelastic conditions, but M_p is not reached.

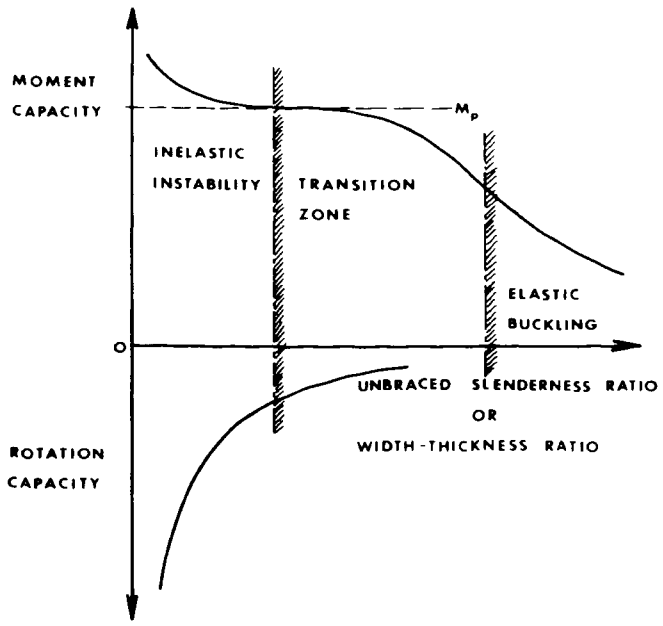

Fig. 2 Schematic variation of moment and rotation capacity with unbraced slenderness ratio and width-thickness ratios.

Sufficient rotation capacity to achieve beneficial moment redistribution under increasing loads exists only in the range where M_p can be reached. Strain-hardening at first-formed hinges may also increase the load capacity of a beam, but in conventional plastic design this is ignored, conservatively, and only adequate rotation capacity is counted on. Allowable stress design uses the elastic and the transition ranges. In the following discussion only beams falling into the range in which plastic design applies will be treated. There has obviously been much work done on beams which are more slender [2-6], but this work does not concern the present study.

In summary, the beams useful for plastic design have the following characteristics: (1) The plastic moment must be capable to be reached and (2) enough rotation capacity must exist so that redistribution of moments can take place. [1-2] It is important to know the limiting maximum values of the unbraced slenderness ratio and the plate width-thickness ratios which bound the region of usefulness for plastic design. It is also important to know the maximum rotation which can be delivered before the moment capacity is reduced by the eventual and unfailing occurrence of lateral and local buckling.

Moment-Rotation Curves of Beams

In the absence of instability effects, a wide-flange beam which is bent in the plane of the web will deform only in the plane of the web. The load-deflection curve, or the moment-rotation curve, can be predicted from the stress-strain curve of the given material, the residual stresses, the cross-sectional dimensions, the longitudinal dimensions and the loads. Integration of the stresses over the cross section, given the moment-curvature relationship and integration of the moment-curvature relationship over the length, gives the load-deformation curve. [1-2] [2-7]

Residual stresses combine with bending stresses to cause yielding. In the early stages

of plastification the beam is slightly less stiff than one without residual stresses. Residual stresses do not, however, affect the magnitude of the plastic moment. [1-2] The strains near the plastic hinges are usually one order of magnitude larger than the strain levels where residual stresses affect behavior, and therefore the residual stresses in plastically designed beams play only a relatively minor role. In contrast, beam-column and column performance is more seriously affected by residual stresses. [2-8] [2-9] The overall performance of beams suitable for plastic design can thus be well predicted by neglecting residual stresses.

Failure of wide-flange beams would take place, theoretically, by tensile fracture when the tensile strength of the material is attained. This type of failure has been observed, sometimes under very artificial conditions. [2-10] In welded frames fracture should be guarded against by avoiding welded connection details which would produce triaxial constraints. Before fracture, and at strains of about one order of magnitude smaller than the fracture strains, a reduction in the moment capacity ("unloading" or "failure") is initiated by the combined occurrence of lateral-torsional and local instability. For beams of practical dimensions this will always be the case. [2-11]

The ideal and the experimental moment-rotation relationship for two types of determinate beams is illustrated in Fig. 3. The top of the figure shows the behavior of a beam containing a segment under *uniform moment*, and the bottom shows the corresponding relationships for a beam under *moment gradient*. The two types of beams are different in that in the upper beam yielding is spread over the whole uniformly bent segment. Whereas for the lower beam, yielding is confined to the region adjacent to the load point.

The best possible in-plane performance of the beam under uniform moment is characterized by the fact that the moment remains constant and equal to M_p while the beam deforms until the average strains in the flanges have reached the strain-hardening strains along the whole region of uniform moment. Only then can the moment be increased above the

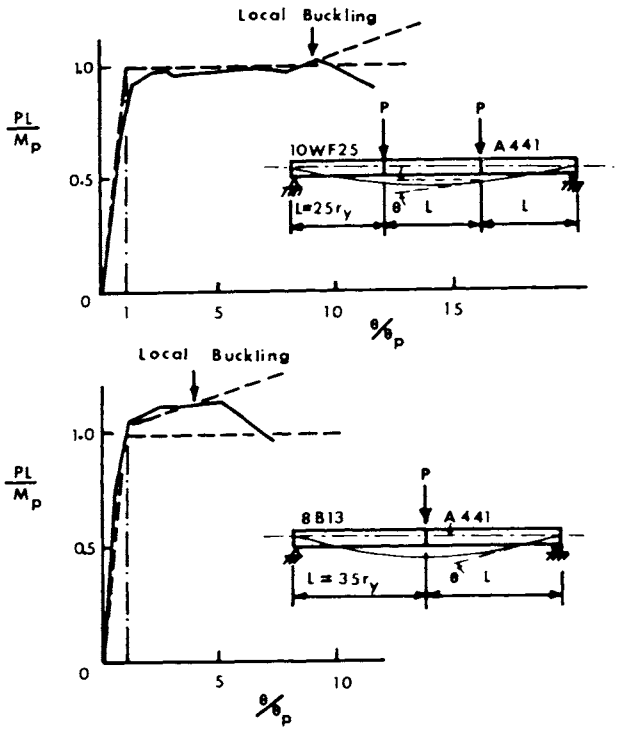

Fig. 3 Experimental and theoretical moment-rotation curves for a beam under uniform moment (top) and a beam under moment gradient (bottom).

plastic moment as strain-hardening takes over (see dashed curve in Fig. 3, upper part). In contrast, yielding in the beam under moment gradient can not spread unless the moment is increased, and so strain-hardening sets in as soon as M_p is reached, resulting in the upward swing of the curve (see dashed curve in Fig. 3).

The experimental curves (solid curves) in Fig. 3 (taken from Ref. 2-12) show that the behavior of these two types of beams follows fairly well the moment-rotation curves predicted by ideal theory until instability takes over and a reduction in moment capacity results.

Because of unavoidable initial crookedness, the unbraced compression flange of the uniformly bent beam segment deflects laterally as soon as M_p is reached. [2-13] This lateral deflection continues to grow as deformation is increased, but the moment capacity is not impaired until local buckles develop in the compressed half of this flange (see arrow on top of curve of Fig. 3).

The midspan moment will increase in the beam under moment gradient due to strain-

hardening. This will continue until a sufficient length of the compression flange has yielded so that a full wavelength of a local buckle can develop. Local buckling will then commence (see arrow in lower part of Fig. 3) and unloading takes place when lateral buckling also sets in.

In both cases both lateral and local instability combine to trigger unloading. Lateral deformation precedes local buckling for beams under uniform moment and the reverse sequence characterizes beams under moment gradient. It also should be noted that the drop in moment is not catastrophic (i.e. dynamic) nor even steep. This drop is rather gentle; at least to moment levels of about 0.8 M_p for the beam tests in Fig. 3.

The general behavior of wide-flange beams, as described above, has been widely observed in experiments on relatively compact statically determinate beams. These characteristics are specifically stated in the test descriptions given in Refs. 2-12 through 2-15 and 2-17 through 2-19, and they are implied in the tests described in Refs. 2-16, 2-20 and 2-21, as well as in many additional tests reported in the literature compiled in Refs. 1-1 and 1-4.

Inelastic instability at average strains, which are an order of magnitude larger than the yield strain, thus seems to limit the ability of steel wide-flange beams to continue to support load with increasing deformation. The combined phenomena of yielding, strain-hardening, in-plane and lateral deformation and local distortion occur soon after the flange is yielded, and they interact so that the separate effects can only be distinguished in a very gross manner. Further complications arise from residual stresses and initial crookedness. It has been impossible to consider all of these effects at once and the instability problem has been solved essentially as two separate buckling problems: local buckling and lateral buckling.

Local Buckling

When a wide-flange steel beam is deformed well into the inelastic range, local buckles appear and eventually the load begins to drop off. Local buckling is either preceded by, or succeeded by, lateral deformations, and it is the combined effect of these two which causes unloading. Unfortunately, it has been impossible to capture this true behavior by a rational analysis. Instead, the problem is treated as a buckling problem where the plate element is considered to remain flat until, under a critical loading, it suddenly buckles.

For the flange, for example, the unbuckled plate element is assumed to be subjected to a uniform longitudinal stress of σ_y, the yield stress and to a strain of ϵ_{ST}, the strain-hardening strain. A theoretical buckling analysis for this state of stress and strain results in width-thickness ratios which are required so that the plate can attain this state.

The first solution to the problem of local buckling in the strain-hardening range was presented by Haaijer (Refs. 2-22, 2-23, 2-24), who recommended the following critical width-thickness ratios for wide-flange shapes:

$$\frac{b}{t} \leqslant 16.6 \text{ and } (d-2t)/w \leqslant 62 \qquad (3)$$

The symbols b, t, d and w denote the flange width, the flange thickness, the total depth and the web thickness of the wide-flange shape. These ratios apply for steel with σ_y = 36 ksi, and they were rounded off to

$$\frac{b}{t} \leqslant 17 \text{ and } \frac{d}{w} \leqslant 70 \qquad (4)$$

in the 1963 AISC Specifications [1-5].

Haaijer's work was based on extensive theoretical and experimental work, and, considering the complexity of the problem, there was fairly good correlation between the two. However, the results do not apply to steels other than ASTM-A36 steel. The wide availability of high strength steels made it necessary to re-evaluate the local buckling problem for these new steels. Based principally on experiments, the British proposed a b/t limit of 15 for their high strength steel (BS 968) [2-25, 2-26] and Massonnet suggested $b/t \leqslant 14$ for the European A52 steel [2-27]. Both of these steels have a yield stress of about 50 ksi. As part of an extensive investigation of the applicability of plastic design for high-strength

steel structures at Lehigh University, [2-12] Lay recommended the following more general formula (Eq. 42 in Ref. 2-28) for the critical width-thickness ratio of the compression flange: [2-28, 2-29]

$$\frac{b}{t} \leq \frac{3.56}{\sqrt{(3 + \sigma_u/\sigma_y)\,(\epsilon_y)\,(1 + h/5.2)}} \qquad (5)$$

where σ_u is the ultimate tensile stress, σ_y is the yield stress, ϵ_y is the yield strain ($\epsilon_y = \sigma_y/E$) and h is the ratio of the elastic to the strain-hardening modulus of the material (Fig. 4). The corresponding b/t ratios for three types of steel are given in Table 1. No comparable formula has yet been developed for the width-thickness requirement of the web, but research on this problem is underway. [2-18] The following interim formula has been proposed [2-1]:

$$\frac{d}{w} \leq 70\sqrt{\frac{36}{\sigma_y}} \qquad (6)$$

where the yield stress σ_y is expressed in units of ksi.

Table 1 shows that the width-thickness ratio requirements become more severe as the yield strength increases. The requirements are not only a function of the square root of the inverse of the yield stress, but also a function of the strain-hardening modulus.

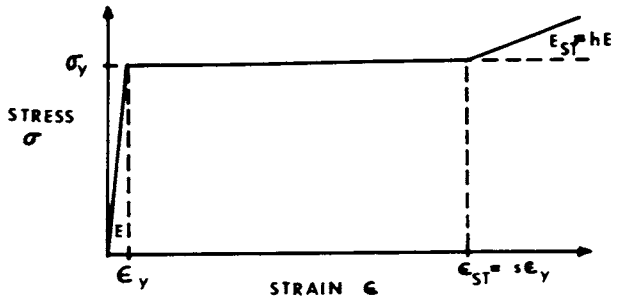

Fig. 4 Idealized representation of initial portions of the stress-strain curve for steel.

The width-thickness ratios of Eqs. 5 and 6 are limiting ratios, and they define a geometric boundary at which the average strains will just be able to reach strain-hardening according to the theory and assumptions which were used. Members with smaller ratios can deform more, and members with larger ratios will deform less. There are some experiments available on both types of members (Refs. 2-22, 2-23 and 2-57) but there is still lacking a rational theory which explains the behavior of members with smaller width-thickness ratios than those defined by Eqs. 5 and 6 and a rational theory which defines the transition, with respect to both strength and deformability, between local buckling at full yielding

Table 1. Critical Width – Thickness Ratios

	A36	A441	A514
σ_u	65 ksi*	78.5 ksi**	120 ksi*
σ_y	36 ksi	54.5 ksi***	100 ksi*
E	29,500 ksi	29,500 ksi	29,500 ksi
ϵ_y	0.00122	0.00185	0.00339
E_{st}	895 ksi**	705 ksi***	146 ksi*
h	33	42	200*
b/t	17.1	13.1	4.7
d/w	70	57	42

* Assumed typical values
** Ref. 2-22
*** Tables 3 and 4, Ref. 2-12

and elastic local buckling. This problem of local buckling certainly deserves further investigation, especially the behavior of beams under different loading conditions and the effect of the whole range of possible practical geometric parameters.

Lateral Bracing Requirements in Plastic Design

The lateral and local deformations are intricately interrelated. It has not been possible to treat these two effects together, and so the lateral deformation problem also has been handled as an individual buckling problem. The end result of such an analysis is a critical maximum spacing of lateral bracing. Lateral buckling of an initially straight unbraced beam segment is assumed to take place at the same instant as local buckling, that is, when the average strain in the compression flange becomes the strain-hardening strain.

The original work on the determination of the required bracing spacing was due to White. [2-30] Additional tests and an evaluation of White's results are given in Refs. 2-20 and 1-1. The current bracing spacing rules in the AISC specifications [1-5] are based on this work. These rules apply, however, only for A36 steel and they are generally conservative. The problem was recently re-evaluated, and more general requirements were formulated as a result. [2-31, 2-32, 2-33, 2-34] According to this research, wide-flange beams in plastic design should be braced according to the following equations:

Beams under Moment Gradient ($-1 \leqslant p \leqslant +0.5$; Fig. 5a)*

$$L_{BR}/r_y = \frac{\pi}{0.7\sqrt{\epsilon_y}\sqrt{1 + 0.7h/(s-1)}} \qquad (7)$$

Beams under Uniform Moment ($+0.5 < p \leqslant 1.0$; Fig. 5b,c)*

$$L_{BR}/r_y = \frac{\pi}{K\sqrt{\epsilon_y}\sqrt{1 + 0.56h}} \qquad (8)$$

In these equations L_{BR} is the unbraced length, r_y is the least radius of gyration of the wide-flange shape, ϵ_y is the yield strain, h is the ratio of the elastic to the strain-hardening modulus, s is the ratio of the strain-hardening strain to the yield strain (Fig. 4) and K is an effective length factor which depends on whether the adjacent span is elastic ($K = 0.54$, Fig. 5b) or yielded ($K = 0.8$, Fig. 5c).

Typical unbraced slenderness ratio requirements are shown in Table 2. For A36 steel and elastic adjacent spans for uniform moment in the critical span, the required unbraced length is 37.5 r_y. This compares with 35 r_y in the AISC specifications. The requirements for high strength steel are again more severe than for A36 steel.

*In Eqs. 7 and 8 the value of the moment gradient separating beams under uniform moment and moment gradient is given as $\rho = 0.5$. This is the value given in the latest reference (Ref. 2-33). Previously a less conservative limit of $\rho = 0.7$ has been suggested [2-1]. The limits in either reference were based on rather arbitrary reasoning. Since no conclusive theoretical or experimental evidence exists to substantiate either limit, and it would probably make very little difference anyway, it is suggested that the practically less severe value of $\rho = 0.7$ be used in design.

Table 2. Typical Unbraced Length Requirements

σ_y	ϵ_y	ρ	K	h	s	L/r_y
36 ksi	0.00122	+1.0	0.54	33	11.5	37.5
36 ksi	0.00122	+1.0	0.80	33	11.5	25.3
36 ksi	0.00122	less than 0.5	–	33	11.5	71.1
54.5 ksi*	0.00185	+1.0	0.54	42*	11.6*	27.2
54.5 ksi*	0.00185	+1.0	0.80	42*	11.6*	18.4
54.5 ksi*	0.00185	less than 0.5	–	42*	11.6*	58.0

*From Ref. 2-22

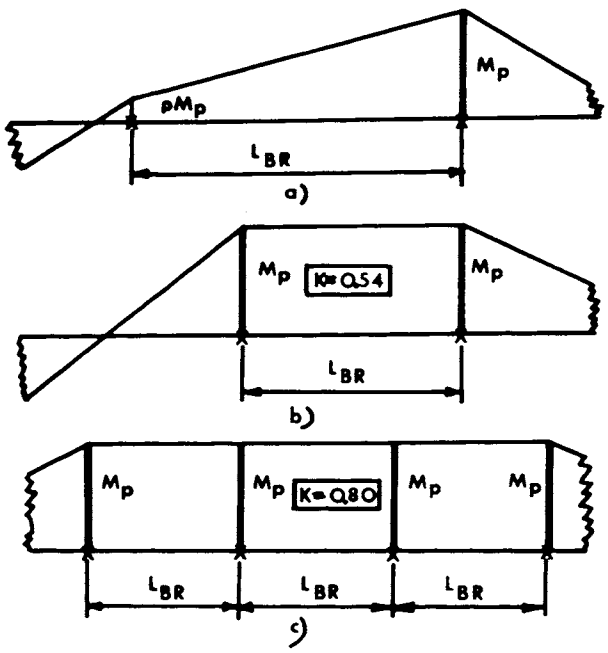

Fig. 5 Typical bending moment diagrams and brace locations.

The width-thickness and bracing spacing requirements given in Eqs. 5 through 8 are designed to insure that the full plastic moment is reached or exceeded and maintained for a sufficiently long rotation.* They apply to all but the last hinge to form in a plastically designed structure. At the last hinge, no rotation is required, and thus the usual rules of conventional design apply for the instability requirements at these hinges.

The usual condition of beams in multistory frames, that is, the top flange continuously supported by the floor slab and the bottom flange restrained by beam connections spaced 7 to 10 ft. on centers, will usually provide adequate lateral bracing. In such cases the only design check is to insure that the beam spacing in the negative moment region does not exceed the limit given by Eq. 7.

Rotation and Energy Absorption Capacity of Beams Under Uniform Moment.

The idealized behavior of wide-flange beams under uniform moment is illustrated in Fig. 6, where a beam with two symmetrically

*The available rotation capacity will be discussed on page 12 et seq.

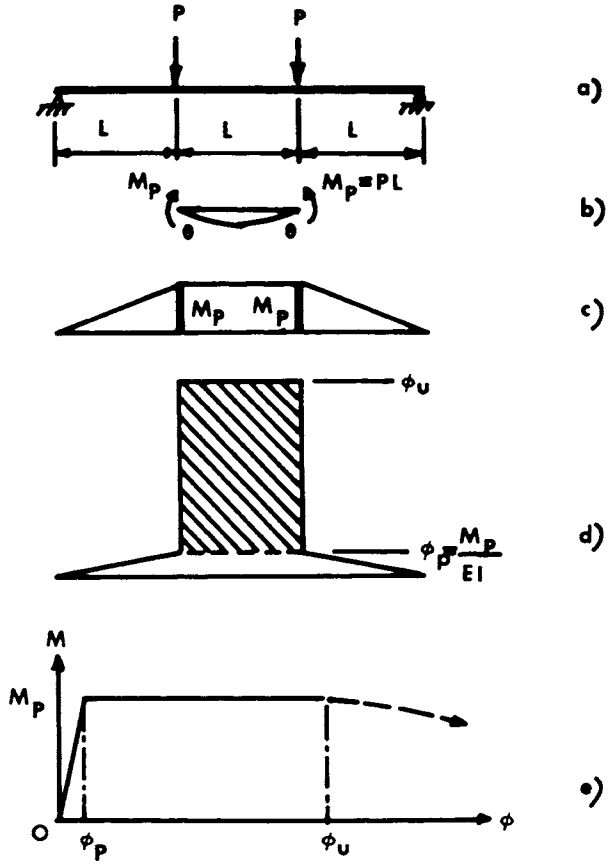

Fig. 6 Behavior of beam under uniform moment.

placed equal loads is shown (Fig. 6a). The central segment is under uniform moment (Fig. 6b). Lateral bracing exists at the supports and under the loads. The central segment is fully yielded and the two outside spans act as elastic restraints. The moment diagram is shown in Fig. 6c, and the corresponding curvature diagram is given in Fig. 6d at the attainment of the maximum curvature φ_u when unloading begins (see idealized M φ curve in Fig. 6e). The rotation θ at the end of the central segment (Fig. 6b) is equal to

$$\theta = \frac{1}{2}\varphi L \tag{9}$$

At the hypothetical start of yielding ($\varphi = \varphi_p$), the end slope is

$$\theta_p = \frac{M_p L}{2EI} = \frac{1}{2}\varphi_p L \tag{10}$$

and at unloading

$$\theta_u = \frac{1}{2}\varphi_u L \tag{11}$$

The rotation capacity is (Eq. 1)

$$R = \frac{\theta_u}{\theta_p} - 1 = \frac{\varphi_u}{\varphi_p} - 1 \qquad (12)$$

and the ductility factor (Eq. 2) is

$$\mu = \frac{\varphi_u}{\varphi_p} \qquad (13)$$

The total energy absorbed per unit length of the segment is approximately equal to the area under the $M-\varphi$ curve, or [2-35]

$$u_T = \frac{M_p^2}{2EI} + M_p\ (\varphi_u - \varphi_p) \qquad (14)$$

Upon release of the load the elastic strain energy is recovered and the approximate energy dissipated in plastic deformation is

$$u_D = M_p\ (\varphi_u - \varphi_p) = \frac{M_p^2}{EI}(1+R) = \frac{M_p^2 \mu}{EI} \qquad (15)$$

The dissipated energy over the whole yielded length is

$$U_D = \frac{M_p^2 L}{EI}(1+R) = \frac{M_p^2 L \mu}{EI} \qquad (16)$$

Equation 16 shows that theoretically the dissipated energy, the rotation capacity and the ductility factor are linearly related to each other.

The rotation capacity R, and thus also U_D and μ at the attainment of the maximum rotation has been determined theoretically from the condition that local buckling and lateral buckling occur simultaneously. The following relationship is given in Ref. 2-32:

$$R = \left[\frac{s-1}{0.7h}\right]\left[\frac{\pi^2}{\epsilon_y \left(\frac{KL}{r_y}\right)^2} - 1\right] \qquad (17)$$

where s, h and ϵ_y are defined in Fig. 4, K is the effective length ratio (Fig. 5) and L/r_y is the unbraced slenderness ratio. The critical unbraced length L_{BR} of Eq. 8 is obtained by setting L_{BR} and $R = 0.8\ (s-1)$ into Eq. 17. The latter value of R represents the *optimum rotation capacity*. If the bracing spacing is less than L_{BR}, the value of R increases above 0.8 $(s-1)$, but will never become extremely large because of combined local and lateral distortion.

Through Eqs. 16 and 17 it is thus possible to theoretically connect the properties of a wide-flange beam to the resulting rotation capacity, the ductility factor and the dissipated energy. There are a number of experiments available against which the theoretical predictions of beams under uniform moment can be tested. The tests reported in Refs. 2-12, 2-13 and 2-14 were chosen for this comparison because they were performed with the main purpose of studying deformability. For all these tests curves relating the applied moment and the resulting curvature are available. To avoid ambiguity of interpretation, the rotation capacity and the energy dissipation were determined to a point equal to 95% of M_p on the unloading part of the curve (Fig. 7). The 95% cutoff is entirely arbitrary and serves only to assure uniform interpretation of the results. Each test was performed on statically determinate beams under two equal concentrated loads (Fig. 6a).

The pertinent test data are listed in Table 3 and the test points are compared with theory in Figs. 8 and 9. The abscissa in these figures is the unbraced slenderness ratio adjusted for the yield strain. The theoretical and experimental rotation capacities are compared in Fig. 8 and the comparisons of the energy absorption capacities are given in Fig. 9. The absorbed energy was obtained by measuring the area under the experimental moment-rotation curves.

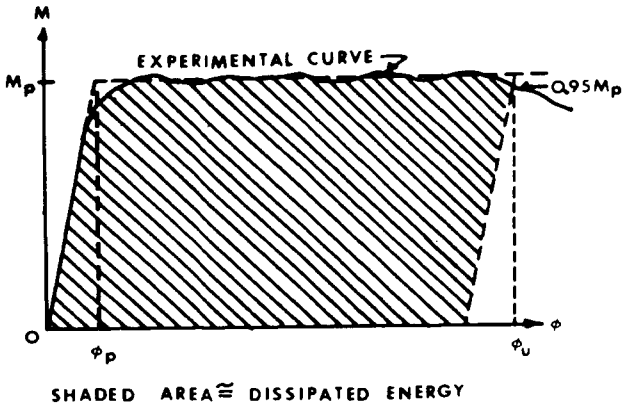

Fig. 7 Rotation capacity and absorbed energy for beams under uniform moment.

Table 3. Experimental Rotation Capacities of Beams (Figs. 8 and 9)

Test	Ref.	$\frac{L_{BR}}{r_y}$	$K_{exp.}$	h	s	σ_y	$\frac{KL\sqrt{\epsilon_y}}{r_y \pi}$	$R_{exp.}$	$\left(\frac{U_D EI}{LM_p{}^2}\right)^*_{exp.}$
LB 11	2-13	35	0.52	33	11.5	35 ksi	0.20	12.8	14.8
LB 15	2-13	40	0.52	33	11.5	35 ksi	0.23	11	12.4
LB 10	2-13	45	0.53	33	11.5	35 ksi	0.26	7	11.9
LB 16	2-13	50	0.54	33	11.5	35 ksi	0.30	5	9.0
G 12	2-14	30	0.80	33	11.5	43 ksi	0.30	4.6	4.2
G 10	2-14	35	0.80	33	11.5	43 ksi	0.34	3.8	3.7
G 9	2-14	40	0.79	33	11.5	43 ksi	0.39	2.6	2.6
G 11	2-14	45	0.78	33	11.5	43 ksi	0.44	1.5	1.7
HT 41	2-12	25	0.52	42	10.5	54 ksi	0.18	10.4	9.5
HT 31	2-12	30	0.52	42	10.5	54 ksi	0.22	6.9	8.7
HT 29	2-12	35	0.52	42	10.5	54 ksi	0.25	4.4	5.6
HT 37	2-12	37.5	0.53	42	10.5	54 ksi	0.27	3.4	4.4
HT 30	2-12	40	0.54	42	10.5	54 ksi	0.30	2.9	3.2
HT 36	2-12	45	0.54	42	10.5	54 ksi	0.34	1.5	3.3

*Determined from the area under the experimental moment-rotation curves.

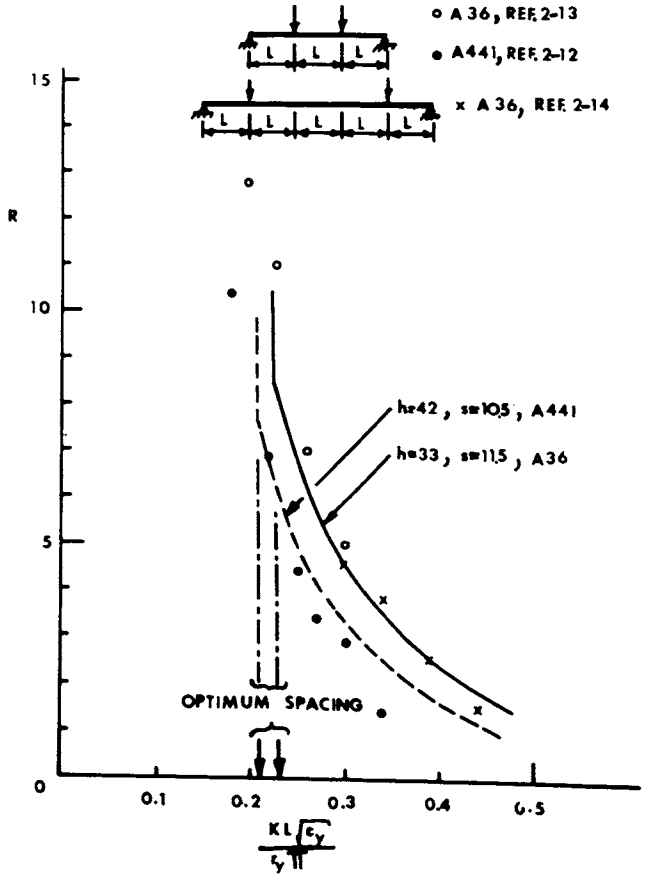

Fig. 8 Comparison of experimental and theoretical rotation capacity.

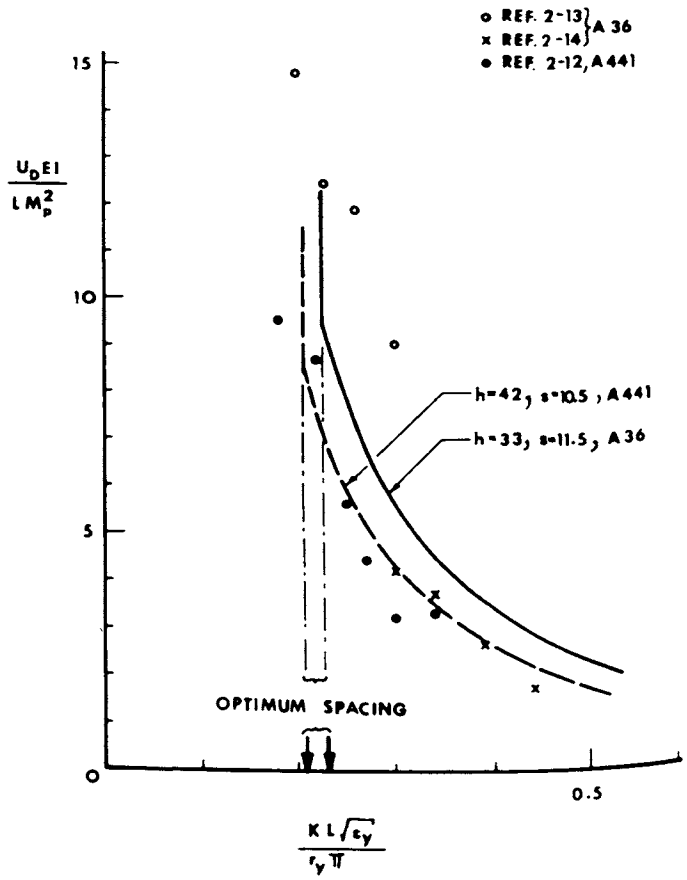

Fig. 9 Comparison of predicted and measured inelastic absorbed energy.

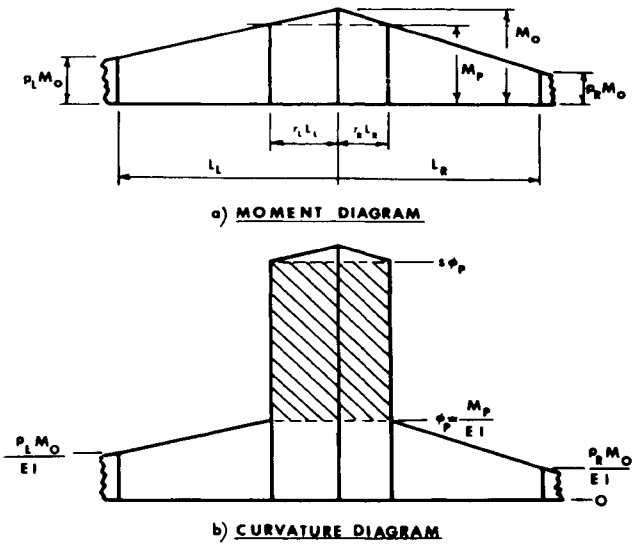

Fig. 10 Moment and curvature diagram at and near a plastic hinge for a beam under moment gradient.

In view of the many idealizations involved in the development of the theory, the correlation shown in these two figures is quite satisfactory. Thus for beams with a uniform moment, it is possible to confidently predict the rotation and energy absorption capacities. It is interesting to note that beams under optimum bracing spacing generally had larger capacities than predicted.

In addition to the tests of Figs. 8 or 9, many more such experiments were reported (Refs. 2-15, 2-36, 2-37, 2-30 and 2-20). Table 4 lists the pertinent results from Refs. 2-15 and 2-20. These tests were performed to study the effectiveness of various types of bracing. It can be seen that rotation capacities of 10 or more are the rule rather than the exception. The average rotation capacity for all beams which were braced to an optimum or near-optimum spacing (Eq. 8) was about 10. In addition, Lay notes in Ref. 2-38 that Massey's tests [2-36] give rotation capacities closely predicted by Eq. 17.

The following conclusions may be drawn from the results presented above: 1) The rotation capacity predictions of Eq. 17 are well substantiated by experiment. 2) "Compact" wide-flange beams (optimum or sub-optimum

Table 4. Experimental Rotation Capacities of Beams

Text No.	Ref.	$\frac{L_{BR}}{r_y}$	σ_y	$R_{exp.}$	$\left(\frac{U_D EI}{M_p^2 L}\right)_{exp.}$
LB-12	2-15	40	34 ksi	21	14
LB-13	2-15	40	34 ksi	18	15
LB-14	2-15	40	34 ksi	12	14
LB-18	2-15	40	34 ksi	12	11
LB-19	2-15	40	34 ksi	11	11
LB-20	2-15	40	34 ksi	12	10
LB-22	2-15	40	38.8 ksi	7	7
P-3	2-15	40	38.5 ksi	12	11
P-4	2-15	40	38.5 ksi	15	12
P-6	2-15	40	38.8 ksi	9	9
P-7	2-15	40	38.8 ksi	8	9
P-8	2-15	40	38.8 ksi	9	10
P-9	2-15	40	38.8 ksi	10	10
P-10	2-15	40	38.8 ksi	6	7
LB-1	2-20	23	32.6 ksi	22	*
LB-2	2-20	41	32.6 ksi	5	*
LB-3	2-20	22	37.6 ksi	5	*
LB-4	2-20	72	32.6 ksi	1	*
LB-7	2-20	29	38.3 ksi	8	*
LB-8	2-20	29	38.3 ksi	9	*

*There were no experimental curves available to the author from which the area under the $M-\varphi$ curve could be determined.

spacing of bracing, and critical or sub-critical width-thickness ratios) deliver a rotation capacity of about 10 or more.

The tests were usually discontinued after only a little unloading had taken place, and so no information is available on the mechanism of unloading. This is also true for the theoretical developments. The trend, however, seems to be that unloading is not rapid but gradual.

No information is available on beams under uniform moment when the load is released and then reversed. Since loading which produces uniform or near uniform moment is primarily due to vertical gravity loading, and this will not reverse during a reversal of the horizontal loads on the frame, the problem is, for this discussion, unimportant.

Rotation and Energy Absorption Capacities of Beams Under Moment Gradient.

Beam segments under concentrated loads and near joints are usually in a region in which the moment varies along the longitudinal axis of the beam. Beams under moment gradient have relatively short zones of yielding, and strain-hardening is present soon after the plastic moment is reached (Fig. 3, lower figure).

Figure 10a shows a portion of a moment diagram near a plastic hinge. The peak moment M_o will exceed M_p because spreading of the yielded zone can occur only in this manner. The length of the yielded zone extends over the region in which the moment is above M_p. The yeilded length τL will depend on the moment ratio ρ to the right and to the left of the plastic hinge. The curvature diagram corresponding to the moment diagram of Fig. 10a is given in Fig. 10b. At $M = M_p$ the curvature jumps from its elastic limit value of φ_p to the strain-hardening curvature $s\varphi_p$, where s is the ratio of the strain-hardening to the yield strain (Fig. 4). Within the yielded zone the curvature will be above $s\varphi_p$.

A conservative estimate of the hinge-angle θ_H is the cross-hatched area in Fig. 10b. This hinge angle represents the inelastic rotation of the plastic hinge. This angle is equal to

$$\theta_H = \varphi_p \ (s-1) \ (\tau_L L_L + \tau_R L_R) \qquad (18)$$

neglecting the triangular area of curvature above $\varphi = s\varphi_p$. Because of this and also for other reasons, the estimate of θ_H from Eq. 18 is about 20% smaller than the true value [2-29, 2-33]. Theoretically the maximum inelastic rotation is reached when either of the yielded lengths $\tau_L L_L$ or $\tau_R L_R$ (Fig. 10a) becomes long enough for one wave length of the local buckle to develop. [2-33] This length is equal to (Eq. 9, Ref. 2-33)

$$\tau_{LB} L = 1.42 b (t/w) (A_w/A_f)^{1/4} \qquad (19)$$

where b, t, w and d are dimensions of the wide-flange cross section and $A_w = (d-2t)w$ and $A_f = bt$ are the web and flange areas, respectively. A combination of Eqs. 18 and 19 leads to the following expression for the theoretically available hinge rotation capacity:

$$\theta_H = 2.84 \epsilon_y (s-1) \left[\left(\frac{bt}{dw}\right) \left(\frac{A_w}{A_f}\right)^{1/4}\right] \left[1 + \frac{V_1}{V_2}\right] \qquad (20)$$

in which V_1 and V_2 are the absolute values of the shears on both sides of the hinge. They are chosen so that

$$V_1 \leqslant V_2 \qquad (21)$$

The last bracket in Eq. 20 allows for the fact that both sides of the hinge may not be yielded to the local buckling limit. The limitations of Eq. 20 are the following:

$$-1.0 \leqslant \rho \leqslant 0.5 * \qquad (22)$$

If $\rho > 0.5$, the formula for uniform moment is to be used (Eq. 17). In order to avoid local crushing under the load point, which is the hinge location, [2-33]

$$V_M \leqslant (M_p/4.8b) (\sigma_u/\sigma_y - 0.88) \qquad (23)$$

where σ_u is the ultimate tensile stress of the material. If V_1 exceeds the value from the

*See footnote with Eqs. 7 and 8.

right side of Eq. 23, the value of V_M is to be used in Eq. 20 instead. Finally, to avoid shear yielding [2-33]

$$V_S \leqslant \frac{A_w\ (\sigma_u + \sigma_y)}{3.46} \qquad (24)$$

If V_2 exceeds the right side of Eq. 24, use the value of V_s in Eq. 20. In the case of a fixed end, or at a point where all yielding takes place in only one member entering a joint, the value of the last bracket in Eq. 20 becomes unity.

The predicted rotations from Eq. 20 are compared to experimentally measured rotations in Table 5 (all but the data from Ref. 2-57 were taken from Ref. 2-33). In addition to basic test data this table contains a comparison of the theoretically predicted and experimentally measured rotations for each of the tests. The recorded test rotation was measured at the point where distinct unloading took place (i.e. the peak of the $M-\theta$ curve in Fig. 3). For all but two of the tests which fulfilled the b/t requirement of Eq. 5

Table 5. Experimental and Theoretical Rotation for Beams Under Moment Gradient

Source Ref.	Test	$\frac{L_{BR}}{r_y}$	$\frac{b}{t}$	$\frac{d}{w}$	σ_y ksi	ρ	θ_H Theory	θ_H Test	Test θ_H ** / Theory θ_H
2-20	LB-5	48	16.9	41.2	38	0.39	0.060	0.082	1.37
2-20	LB-6	38	16.9	41.2	38	0.71	0.066	0.130	1.97
—	G-1	47	14.9	43.5	42	0.5	0.057	0.064	1.12
—	G-2	56	14.9	43.5	42	0.5	0.057	0.058	1.02
—	G-5	56	14.9	43.5	42	0	0.057	0.044	0.77
2-39	T-5	60	13.6	45.2	36	0	0.059	0.071	1.20
2-40	1	32	9.20	23.8	36	0	0.074	0.095	1.29
2-12	HT28	35	15.7	34.8	54	0	0.052	0.074	1.42*
2-12	HT43	23	15.7	34.8	54	0	0.034	0.039	1.15*
2-12	HT52	72	15.7	34.8	54	0	0.084	0.086	1.02*
2-16	5	25	13.9	32.8	41	0	0.091	0.162	1.78
2-16	6	35	13.9	32.8	41	0	0.09	0.168	1.85
2-16	9	32	13.9	20.8	42	0	0.142	0.370	2.60
2-16	12	38	10.2	41.0	38	0	0.051	0.100	1.96
2-16	15	35	14.0	45.5	39	0	0.072	0.130	1.80
2-16	18	43	17.7	59.6	33	0	0.050	0.026	0.52
2-16	21	32	18.4	27.8	41	0	0.141	0.161	1.14*
2-57	A-1	35	18.8	32.7	41	0	0.067	0.113	1.69*
2-57	A-2	35	16.3	32.7	41	0	0.060	0.122	2.03
2-57	B-1	35	19.4	45.0	54	0	0.098	0.028	0.29*
2-57	B-2	35	14.0	45.0	54	0	0.077	0.049	0.64*
2-57	B-3	35	16.3	45.0	54	0	0.086	0.052	0.61*
2-57	B-4	35	17.8	45.0	54	0	0.092	0.030	0.33*
2-57	B-5	35	18.3	45.0	54	0	0.094	0.030	0.32*
2-57	C-1	35	19.4	54.5	53	0	0.065	0.024	0.37*
2-57	C-2	35	14.0	54.5	53	0	0.051	0.048	0.94*
2-57	C-3	35	16.3	54.5	53	0	0.057	0.030	0.53*
2-57	C-4	35	17.1	54.5	53	0	0.061	0.022	0.36*
2-57	C-5	35	17.8	54.5	53	0	0.059	0.032	0.54*

* b/t exceeds limit defined by Eq. 5.
** Average ratio of test to theory, excluding tests marked by *: 1.52. Average ratio of test to theory, all tests: 1.12.

the test rotation exceeded the predicted rotation with the average over prediction of about 50 per cent. This is more than the estimated conservatism in Eq. 20. The reason for this is the frequently observed fact that the moment capacity does not immediately drop off after the first observed local buckle. This can be seen in the lower curve of Fig. 3 where unloading commences after local buckling. Since the theory is based on the first occurrence of local buckling, it is unable to predict what happens after it. Unfortunately there is no theory available yet to predict post-local buckling performance.

On the 15 tests in Table 5 for which the b/t requirements of Eq. 5 were not fulfilled, five tests showed somewhat higher measured rotations than predicted. For these tests the b/t limit was not greatly exceeded. On the other hand, tests with very slender flanges showed very little rotation capacity.

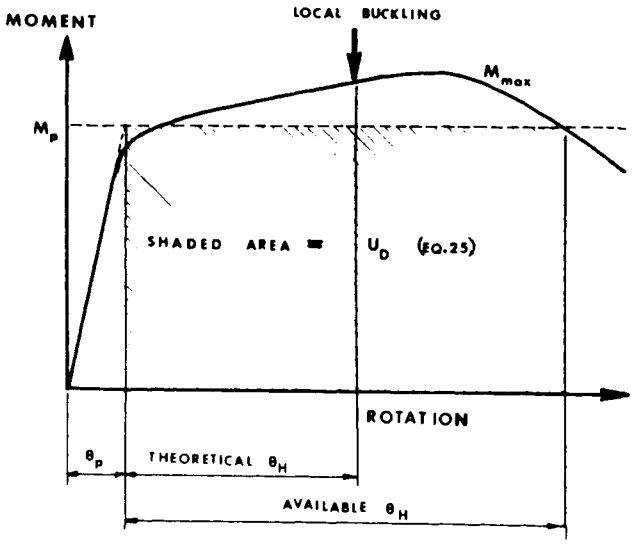

Fig. 11 Schematic moment-rotation curve of beams under moment gradient.

In plastic design, the increased moment due to strain-hardening is usually neglected, and the level of expected moment capacity is the full plastic moment, M_p.* On the schematic drawing of Fig. 11 it is seen that, whereas the theoretical rotation capacity stops at the onset of local buckling, the available capacity is much greater. Unfortunately there are very few tests for which the value of the rotation down to M_p on the unloading part of the curve is available. The tests listed in Table 5 also had closer bracing spacing than is required by Eq. 7.

In general, the tests reported in Ref. 2-16 (see Table 5) had a greater average underprediction of θ_H than the other tests. This could be due to the fact that the load and deformations were read "on the run", without stopping at each load increment, as was done for the other tests. This may indicate that the faster load application may have a beneficial effect on θ_H. This fact could be of great importance to beams in a frame designed to resist earthquakes. More research on this aspect of the problem is definitely needed.

In conclusion, θ_H as predicted by Eq. 20 seems to give a conservative estimate of the rotation capacity of beams under moment gradient. Further research needs to be done on the following topics: 1) A theory is needed on the post-local buckling deformation behavior; 2) tests are needed to get more complete moment-rotation curves, especially for the region beyond local buckling; 3) tests are needed to study the $M-\theta$ relationship for beams braced in accordance with Eq. 7, that is, tests on beams with longer unbraced lengths; 4) tests and theoretical work are needed on the effect of the rate of loading.

It should be noted here that the state of knowledge with regard to the available rotation capacity, the required bracing spacing and the flange width-thickness ratios for beams under moment gradient still is quite incomplete, both with regard to theory and tests. There is no really conclusive separation between beams under uniform moment and beams under moment gradient, and this leads to contradictions and inconsistencies. There is no theoretical relationship connecting the width-thickness ratio, the bracing spacing and the available hinge angle θ_H. The relationship defined by Eq. 20 applies theoretically only to beams having the bracing spacing of Eq. 7 and the b/t ratio of Eq. 5. That rotation capacity increases with a decrease of the b/t ratio was demonstrated experimentally by Lukey and

*An exception to this approach is the newly proposed method due to Lay, which includes strain-hardening [2-41].

Adams [3-57], but there is no theory to explain this. Also, θ_H from Eq. 20 is quite conservative.

There are also a number of practical questions which need to be considered: 1) What takes place in the negative moment region of a beam welded to a column? 2) Does statical indeterminacy have any influence?

The theory presented here represents the first steps toward a solution of these problems. Much work still needs to be done before the complete problem is solved. However, the results presented here are the best available, and they are, in general, conservative. In view of the lack of a more perfect theory, they can be used with confidence in design. The results will now be used to determine the dissipated energy of beams under moment gradient.

The energy dissipated during hinge rotation is equal to the area under the $M-\theta$ curve, or, approximately and conservatively

$$U_D = M_p \theta_H \tag{25}$$

In this expression the contribution above M_p is neglected, and θ_H is the conservative estimate of the inelastic rotation from Eq. 20. The energy from Eq. 25 is the available energy per each plastic hinge up to the point of local buckling.

The available hinge angle θ_H, and thus also the available energy (Eqs. 20 and 25, respectively) depend on material properties (s, ϵ_y), cross sectional properties (b, t, d, w), the ratio of the shears adjacent to the hinge, V_1/V_2 and the moment ratios (ρ_1 and ρ_2).

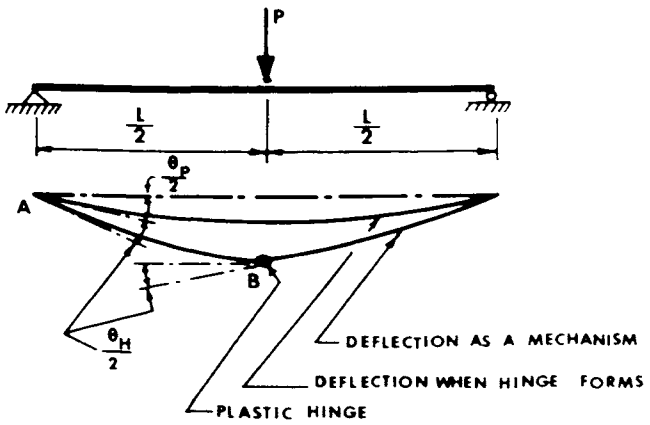

Fig. 12 Motion of a simply supported beam with a plastic hinge.

The inelastic hinge-rotation θ_H is expressed in units of radians in Eq. 20. In general it is not possible to express a non-dimensional numerical ratio, such as was possible for the beam under uniform moment, to give a rotation capacity R or a ductility factor, μ, which is only the function of the material and the bracing spacing. The dimensions of the cross section and the overall dimensions of the structure also enter into the picture. This is illustrated on the simply supported beam under a central concentrated load in Fig. 12.

The ductility factor μ is defined as (Eq. 2)

$$\mu = \frac{\theta_u}{\theta_p} \tag{26}$$

In terms of the rotation of Fig. 12,

$$\mu = \frac{\theta_p/2 + \theta_H/2}{\theta_p/2} = 1 + \frac{\theta_H}{\theta_p} \tag{27}$$

The elastic rotation, θ_p, when the maximum moment equals M_p at the center of the beam is equal to

$$\theta_p = \frac{M_p L}{2EI} \tag{28}$$

Since

$$\frac{M_p}{EI} = \varphi_p \approx \frac{2\epsilon_y}{d} \tag{29}$$

the ductility factor becomes

$$\mu = 1 + \frac{\theta_H d}{\epsilon_y L} \tag{30}$$

Substitution of θ_H from Eq. 20 gives

$$\mu = 1 + 2.84 \left(\frac{d}{L}\right) (s - 1) \left[\left(\frac{bt}{dw}\right) \left(\frac{A_w}{A_f}\right)^{1/4}\right] \left[1 + \frac{V_1}{V_2}\right] \tag{31}$$

If average values of $s = 11.0$, $\frac{bt}{dw}\left(\frac{A_w}{A_f}\right)^{1/4} = 0.7$ (Ref. 2-42 lists the values of this parameter for rolled wide-flange shapes; it varies from about 0.5 to 0.9) are substituted into Eq. 31, and if it is noted that the last bracket equals 2.0 for the beam of Fig. 12, then

$$\mu = 1 + \frac{40}{L/d} \tag{32}$$

Thus for a given section and loading condition the ductility factor depends only on the L/d ratio of the beam. Assuming, for example, L/d = 16, the ductility factor becomes equal to 3.5. Because of the reasons given above, the ductility factor of a test beam should exceed this value by at least 40 per cent; thus one could expect that μ = 5 would be a reasonable ductility factor for this beam.

The foregoing has shown that it is possible, for specific instances where all the information about a beam is known, to define a ductility factor. However, the variety of parameters entering into the determination of μ is so large, that it seems advisable to define hinge-rotation in terms of θ_H, in radians (Eq. 20). This available hinge angle will be compared with the required hinge angle for indeterminate structures in Chapter 6.

Beams Under Load Reversal

The previous discussion concerned beams under monotonic loads, i.e., the beams were loaded once and in only one direction. The information was obtained from tests made in support of plastic design which is based on the assumption of monotonic and proportional loading. For nominally statically loaded structures this assumption may be theoretically questioned, although a good case has been made for static loading on the basis of shakedown studies [1-1]. For structures subjected to earthquake motion, the assumption of monotonic and proportional loading is unacceptable. Beams in such structures will be subject to load reversals which cause several excursions into the inelastic range in both directions of bending. [2-43] It is thus necessary to know the behavior of beam under reversed loading, where the load reversals deform the beam repeatedly into the inelastic range. Unfortunately little theoretical work and only very few experiments are available.* A search was made of the available literature, especially the Proceedings of the World Conferences of Earthquake Engineering (Berkeley, 1956; Tokyo, 1960; New Zealand, 1965). The only relevant work was found to be that at the University of California at Berkeley (Refs. 2-44, 2-45, 2-46) and two tests performed under the supervision of the author [2-47]. There are many references on the behavior of steel (the material) under cyclic inelastic tension or bending (see, for example, the survey presented in Ref. 2-48 and the work in Refs. 2-49 through 2-56). And, it is well understood that the material itself has a stable and well-defined hysteresis loop, and that failure eventually occurs by fracture due to low-cycle fatigue. However, because of effects of local buckling and lateral deformations, a knowledge of material behavior alone is not enough to determine the behavior of a whole member.

In the Berkeley tests, short, cantilevered wide-flange beams were loaded at their ends by a concentrated load which reversed its direction and which bent the beams in the plane of the web. Two series of tests were performed: In the first series of tests 35-in.-long 4M13 beams (L/r_y = 37; b/t = 10.5; σ_y = 41 ksi) were fully clamped at the fixed ends [2-44]. In the second series 8W20 beams of 66-in. length (unbraced slenderness ratio of 27.5, b/t = 14 and σ_y = 39 ksi) were attached by moment connections to a short 8W48 column section [2-45, 2-46]. The inelastic behavior in each of these tests was essentially the same. Local buckling occurred in the compressed flange but no drop-off of moment capacity was experienced as the beams were loaded well into the strain-hardening range in one direction. Upon removal of the load and re-application in the other direction, the local buckles were straightened out on the previously compressed flange as new local buckles occurred on the reverse compressed flange. Failure finally occurred due to low-cycle fatigue in the zones of local buckling. Up to fracture the load-deformation curves experienced remarkable stability, each curve falling right on the curve from the previous cycle. No lateral buckling was observed at any stage of the tests.

An examination of the inelastic rotations of the tests (Refs. 2-44 and 2-45) showed that the beams were rotated to about 40 per cent

*There probably are many more tests than the author is aware of, especially in the literature of Japan and the Soviet Union.

more than the rotation predicted by Eq. 20. The beams in these tests, as well as the connections by which they were attached to the stub-column, behaved extremely well. This shows that steel wide-flange beams under reversed loading can be reliably counted on to deform inelastically, thus absorbing a predictable amount of energy without loss of moment capacity.

The Berkeley tests are very important pilot tests. However, further tests with a larger range of variables are needed. The flange and web slenderness (b/t and d/w ratios) and the bracing spacing were all subcritical when compared to the requirements of Eqs. 5, 6 and 7. The important question as to what these critical requirements are was not answered experimentally and no attempt has been made at a theoretical solution. It is obvious that the theory for monotonic loading (Eq. 20) is conservative. Is it even more conservative for reversed slow quasi-static loading? What effect does the rate of loading have?

One of the tests reported in Ref. 2-47 (where wide-flange beams were tested as beams under a reversible central concentrated load) had a bracing spacing somewhat larger than that recommended by Eq. 7. Although the beam was subjected only to one-and-a-half cycles of loading, it was apparent that its moment and rotation capacity were deteriorating due to combined local and lateral buckling. Thus not all beams behave as the beams in the Berkeley tests.

The behavior of steel beams under cyclic reversible loads in the inelastic range deserves further study. The following research is recommended:

1) Experiments on beams with larger width-thickness ratios and unbraced lengths should be performed to experimentally determine the critical values of these parameters.

2) Theoretical studies should concentrate on a better and more inclusive prediction of behavior than is now possible. Such studies should deal with the post-buckling behavior, with the full range of width-thickness ratios and bracing spacing, with strain rate and dynamic effects and with a clear definition of what constitutes satisfactory and unsatisfactory behavior under reversed loading.

3) A correlation should be sought between the material behavior, including cumulative damage and low-cycle fatigue failure, and the behavior of a real beam in a real structure.

4) The inelastic behavior of composite continuous beams and A572 beams should be investigated.

3. BEAM – COLUMNS

Beam-colums are members which are subjected to appreciable amounts of both axial load and bending moments. In multistory frames all the vertical members and in some instances even some horizontal members can be considered as beam-columns. In general, beam-columns may be bent about both principal axes, and forces producing bending may be present at the ends and in the span. In the usual column framing, however, only end moments are present, and these act about the principal axis of the member. Most of the research has been performed on the simplest situation: beam-columns with end-moments only about the principal axis of the wide-flange section. Not too much work has been performed on beam-columns bent about the weak axis. The following discussion will concentrate on this problem, although beam-columns with inter-panel loading and biaxial loading will also be briefly considered. A great deal of work has been performed on inelastic steel beam-columns, and in some respects more is known about such members than about the apparently simpler beams.*

A beam-column and its loading is shown in Fig. 13. The loading consists of an axial load P and moments M_o and βM_o, where β is the ratio of end moments and it is chosen such that $-1 \leqslant \beta \leqslant +1$, a value of $\beta = +1$ indicating two equal end moments which cause single curvature bending. If the axial load P is applied first and then M_o is increased from zero, the member will deform as shown in

*Unfortunately not a great deal is known about very heavy beam-columns (14 W 426 or the jumbo sizes). Their behavior may be somewhat different than the behavior discussed here.

Fig. 13. A usual measure of this deformation is the end rotation θ. The highest possible moment which can be attained is the fully plastic moment, M_{pc}, where the cross section is fully yielded under the end moment and the axial force. [3-1] A good estimate of this "reduced plastic moment" is

$$M_{pc} = 1.18M_p\,(1 - P/P_y) \text{ for } P/P_y \geqslant 0.15 \tag{33}$$

for wide-flange members bent about the strong axis. In this equation M is the plastic moment of the section under zero axial force and $P_y = A\sigma_y$, is the fully plastic load.

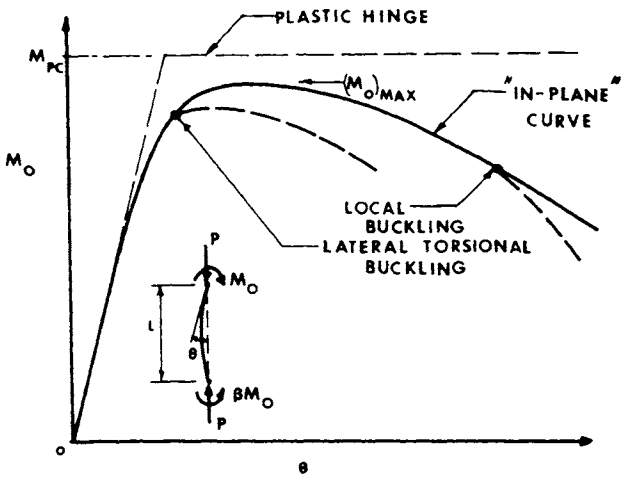

Fig. 13 Schematic moment-rotation curves for beam-columns.

It may not be possible for the beam-column to achieve M_{pc}, although in many practical cases M_{pc} can be reached [3-2]. The reduction in moment capacity is due to the combined effect of the "secondary" moments introduced by the axial force times the deflection, and the reduction of the flexural stiffness due to yielding. The heavy solid curve in Fig. 13 is the resulting $M_o - \theta$ curve. Due to yielding and second order bending, the moment will reach a peak, and thereafter it will have to be reduced to maintain equilibrium upon further bending. The reduction in both moment and rotation capacity is purely an "in-plane" phenomenon and it differentiates the performance of a beam-column from that of a beam. Out-of-plane effects, such as lateral-torsional buckling and local buckling, further tend to reduce the capacities of the beam-column (see dashed curves in Fig. 13).

In-Plane Deformation Capacities of Beam-Columns

The attainment of a peak point on the $M_o - \theta$ curve is a form of instability and it requires that portions of the beam-column be yielded. [3-3] Because of the nature of the wide-flange cross section, and because of the important influence of residual stresses [3-3], the determination of the $M_o - \theta$ curve is performed by numerically integrating the moment-curvature relationship. This numerical integration procedure is very simple in concept, but because of its repetitious nature it is best suited for computer solution. Two frequently used methods of numerical integration are described in Refs. 3-3, 3-4, and 3-5. In these references the considerable amount of research performed on the behavior of in-plane beam-columns is also described and referenced.

The construction of the $M_o - \theta$ curves is most efficiently performed by the use of "column-deflection-curves." The description of the steps from the moment-curvature relationship to the $M_o - \theta$ curves, via the numerical integration procedure and the column-deflection curves, is available in many references and will therefore not be repeated here(e.g., Refs. 3-4 through 3-7).

For the purposes of this discussion it is only important to know that efficient computational tools exist whereby the in-plane load-deformation relationship of beam-columns, including the unloading portion of the curve, can be obtained. Furthermore it is important that for steel wide-flange beam-columns bent about their major axis the load-deformation curves are for all practical purposes identical for all wide-flange shapes, with only the following variables differentiating the different cases of bending and length: M_o/M_p (or M_o/M_{pc}), P/P_y, L/r_x (the strong axis slenderness ratio), β (the end moment ratio), θ and σ_y. Interaction curves relating P/P_y and M_o/M_p for given values of L/r_x, β and σ_y at the maximum moment condition are given as curves, tables, and in algebraic formulas (ob-

tained by curve fitting from the interaction curves) in Refs. 3-1, 3-3, 3-5, 3-8 and in the Appendix to Part 2 of the AISC Specification [1-5]. End moment versus end rotation curves are given for most practical combinations of P/P_y, L/r_x and β in Refs. 3-9 and 3-10. Excellent experimental correlation with predicted strengths and with predicted $M_o - \theta$ curves exists for steel wide-flange and steel box columns and this correlation is documented in Refs. 2-12, 3-3, 3-11, 3-12, and 3-13.

The status of knowledge on the behavior of beam-columns which are bent in a principal plane of the cross section and which are forced by bracing to deform in this plane is thus fairly complete both from a theoretical as well as from an experimental point of view.

Since the peak part of the $M_o - \theta$ curve (solid curve in Fig. 13) is usually rather flat, the rotation corresponding to $(M_o)_{max}$ is poorly defined. Rotation capacity is therefore defined with reference to the rotation θ_u corresponding to 95 per cent of $(M_o)_{max}$ on the unloading portion of the curve, the same way as was done in Fig. 7 for beams. The rotation capacity is thus

$$R = \frac{\theta_u}{\theta_p} - 1 = \mu - 1 \qquad (34)$$

where θ_p is the elastic rotation of the beam-column end at $M_o = 0.95\ (M_o)_{max}$. The experimentally measured rotation capacities and the corresponding theoretical values are given for several tests in Table 6. [3-15] The tests marked "local buckling" were adjusted for this

Table 6. Experimental and Theoretical Rotation Capacities of Beam-Columns

Ref.	Test No.	Member	L/r_x	P/P_y	β	Type of Failure	Rotation Capacity Experiment	Theory
3-11	A2	8WF31	55	0.65	0	Bending	1.1	1.2
3-11	A3	8WF31	55	0.32	0	Local Buckling	3.3	2.6
3-11	A4	8WF31	55	0.49	0	Bending	1.6	1.9
3-11	A5	4WF13	110	0.33	0	Bending	0.5	0.5
3-11	A6	4WF13	112	0.50	0	Bending	0.3	0.4
3-11	A7	4WF13	112	0.16	0	Bending	1.4	1.2
3-11	A8	8B13	52	0.30	0	Lateral Buckling	1.8	2.8
3-11	A9	8B13	52	0.12	0	Local Buckling	3.1	2.0
3-11	A10	8B13	52	0.60	0	Lateral Buckling	1.9	1.4
3-12	RC1	8WF31	59	0.50	1.0	Bending	0.9	0.8
3-12	RC2	8WF31	59	0.40	1.0	Bending	1.8	1.2
3-12	RC3	8WF31	60	0.42	1.0	Bending	0.7	1.1
3-12	RC4	8WF31	40	0.57	1.0	Bending	1.8	1.5
3-12	RC5	8WF31	40	0.56	1.0	Bending	2.6	1.5

effect (see discussion below), but the tests which failed by in-plane bending and lateral buckling were determined from the numerical integration procedure, considering only in-plane behavior.

Comparison of the two rotation capacity values in Table 6 gives reasonable agreement. It should be noted that the rotation capacities are relatively small when compared to beams. This is not always the case, especially for short beam-columns under light axial loads. The available test results given in Table 6 are for relatively long beam-columns, and they do not possess much inelastic deformability.

Rotation capacities of the order of 4 to 13 were reported on model tests on ¾-in.-deep wide-flange sections of 8- to 22-in. length loaded with one end moment [3-14]. The test specimens were pieces of annealed steel glued together, and the maximum flange width-thickness ratio was about 4.

Theoretical curves relating the axial load ratio P/P_y, the rotation capacity R and the slenderness ratio L/r_x are given in Figs. 14 and 15 for the loading case of two equal end moments ($\beta = +1.0$, Fig. 14) and for the case of one end moment ($\beta = 0$, Fig. 15). These curves apply for steel wide-flange beam-columns bent about their strong axis and $\sigma_y = 36$ ksi. They apply only to in-plane performance, except that they are adjusted for the possibility of local buckling. The rotation capacity is defined as in Eq. 34 where θ is either the rotation to 95 per cent of $(M_o)_{max}$ on the unloading branch of the $M_o - \theta$ curve or the rotation at which buckling sets in, if local buckling occurs first [2-29].

The criterion of local buckling used in obtaining the curves in Figs. 14 and 15 was the attainment of a strain equal to the strain-hardening strain over a sufficiently long segment of a flange so that one full wavelength of the local buckle could develop. The curves in Figs. 14 and 15 were determined by searching for the regions in the column-deflection-curves in which this condition of local buckling takes place.* For the case of $\beta = 0$ (Fig. 15), it is possible that a plastic hinge forms at the end of the beam-column. In this case the end rotation is determined as for a beam, and a modified form of Eq. 20 is used [2-29].

The rotation capacity values for Figs. 14 and 15 thus include both in-plane instability and local buckling. They assume, however, adequate lateral bracing. When the beam-column has two equal end moments ($\beta = +1.0$, Fig. 14), very little rotation capacity exists for slenderness ratios larger than about 30 to 40. Therefore, such members do not absorb a great deal of energy, and they should probably

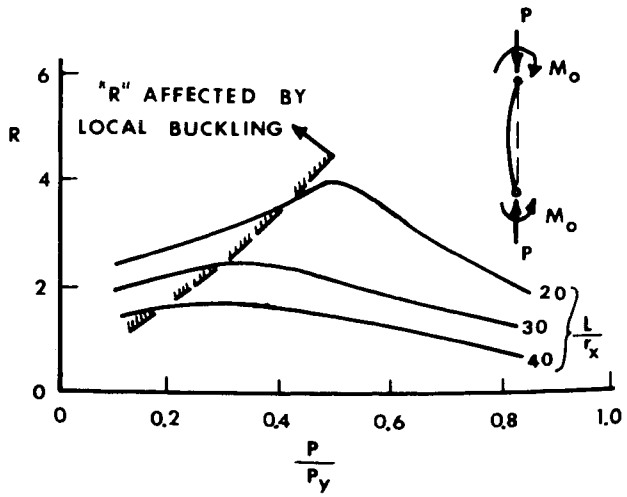

Fig. 14 Rotation capacity of beam-columns, $\sigma_y = 36$ ksi, $\beta = 1.0$.

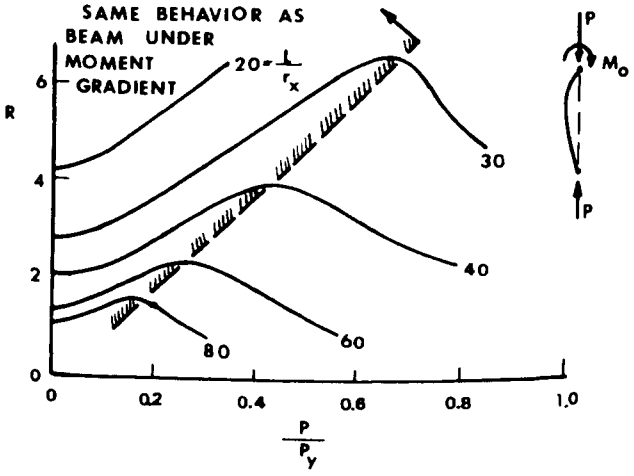

Fig. 15 Rotation capacity of beam-columns, $\sigma_y = 36$ ksi, $\beta = 0$.

*The curves in Figs. 14 and 15 were taken from Ref. 2-29, and the method of constructing them is described in Ref. 3-15, where, however, overly conservative results are presented. Even so, the local buckling cut-off in Fig. 14 is conservative. Local buckling for beam-columns of compact shape has not been experimentally observed to reduce rotation capacity at a moment of 0.95 $(M_o)_{max}$ on the unloading branch of the curve.

not be counted on to do so. Such a loading would not occur under seismic loads anyway. The rotation capacity of beam-columns with only one end moment is quite substantial, especially for shorter members ($\beta = 0$, Fig. 15). Rotation capacities of 6 (or ductility factors of 7) are not uncommon for practical beam-columns. For the case of beam-columns under double curvature moment ($\beta \approx -1$), which is a typical situation for multistory frames subjected to earthquake loads, one-half of the slenderness ratio of the member should be used when determining the rotation capacity from Fig. 15.

The information in Figs. 14 and 15 is rather incomplete. However, the $M_o - \theta$ curves in Ref. 3-10 could be used directly to obtain the maximum rotation θ_M, the elastic rotation θ_p and the maximum end moment $(M_o)_{max}$. The rotation capacity, R, the ductility factor μ, and the inelastic energy absorption capacity.

$$U_D = (\theta_u - \theta_p)\ (M_o)_{max} \qquad (35)$$

could then be computed. Because of the many variables involved, it is difficult to make more general statements about the energy absorption capacity. Eq. 35, however, provides the means whereby this value can be determined in any individual case. The $M_o - \theta$ curves in Ref. 3-10 terminate at the start of local buckling, so this restriction is already taken care of.

In-plane beam-column behavior as described above depends on the presence of adequate lateral bracing to prevent the occurrence of lateral-torsional buckling. There has been little systematic research performed yet, as in the case of beams, to recommend rules for adequate bracing spacing. However some thought has been given to this problem in Refs. 2-29 and 3-2, where it was concluded that the bracing spacing requirements for beam-columns are probably not as stringent as for beams. However, it has been recommended [3-2] that for $0 \leqslant \beta \leqslant +1$ the bracing should be spaced according to Eq. 8. For $-1 \leqslant \beta < 0$ the same equation should be used, except that the more liberal Eq. 7 applies if

$$\frac{P}{P_y} \leqslant \frac{1 - (L/r_x)\ (\sqrt{\epsilon_y}/\pi)}{1 + (L/r_x)\ (\sqrt{\epsilon_y}/\pi)} \qquad (36)$$

These bracing rules are quite conservative and further work should result in more liberal provisions.

For flanges the maximum recommended width-thickness ratio is determined by Eq. 5. For webs the recommended width-thickness ratio is [3-2]

$$d/w \leqslant (70 - 100P/P_y)\sqrt{36/\sigma_y} \qquad (37)$$

$$d/w \leqslant 42\ \sqrt{36/\sigma_y} \qquad (38)$$

Lateral-Torsional Buckling of Beam-Columns

Inadequately braced beam-columns will fail by lateral-torsional buckling before the in-plane maximum moment is reached. This is shown schematically in Fig. 13. The critical moment causing lateral-torsional buckling can be determined by standard elastic methods of analysis [3-21]. The critical moment can also be determined if lateral-torsional buckling occurs after some parts of the member have already yielded (e.g., Refs. 3-16 through 3-20). However, no analysis has yet been presented for the load-deformation path beyond the start of buckling. Thus it is possible to assess the strength at the onset of buckling, but no analytical information is available on the post-buckling deformability of the beam-column. There are, however, a number of experiments which were performed on unbraced wide-flange beam-columns (see Refs. 3-11, 3-14, 3-15, 3-17, 3-18 and 3-19). These experiments were performed over a wide range of P/P_y and L/r_y values and for $\beta = -1$, 0 and +1, and they quite conclusively show that very little rotation capacity is available if failure is by lateral-torsional buckling. Most of these tests showed a rotation capacity of 2 or less, although in some isolated instances it was larger. In view of the lack of an adequate post-buckling theory, it has been recommended that beam-columns which do not meet the bracing requirements stated above should not be counted on to deliver any inelastic rotation capacity. [3-1] [3-5]

Further Topics on Inelastic Beam-Columns

The in-plane rotation capacity of beam-columns loaded by end forces and inter-span

transverse forces has not yet been examined in detail, although ultimate strength interaction curves (Refs. 3-22, 3-23) and some moment-rotation curves are available [3-24]. The problem of obtaining this information is not very great because the same method of numerically integrating the moment-curvature relationship applies as for beam-columns without lateral load.

In contrast, the problem of the biaxial bending of beam-columns is of great practical interest. Unfortunately, the great complexity of the problem has not yet permitted the development of more than a few isolated analytical and experimental results. [3-25, 3-26] The major emphasis in both the analytical and the experimental work has been on strength rather than on deformability. Therefore it is not possible to draw any conclusions about the deformation capacity of biaxially loaded beam-columns. Several universities are working on this problem under the guidance of a Task Committee of the Column Research Council, and it is expected that considerably more will be known about this topic in the near future.

There is no publication on either tests or analytical work known to the author on the behavior of beam-columns under reversed loadings. This is indeed a very timely and important research topic.

The work on the in-plane behavior of steel beam-columns assumed that inelastic straining always proceeds in its initial direction. It was also assumed that the axial load remains constant while the end moment changes. In the inelastic range, the deformation path depends on prior history, and the idealized assumptions stated above certainly do not hold true for a beam-column in a frame. Some attempts have been made to examine these assumptions in Ref. 3-6, and it was shown that their effect on over all behavior was negligible, at least for the cases which were considered. There is further need to thoroughly investigate the effects of the path by which forces, deformations and strains arrive at any particular position.

Research Needs

The following brief list gives several of the research needs on topics on the inelastic deformability of steel beam-columns:

1) Experimental and analytical studies on the behavior of beam-columns under reversing end moments will give information on the design of earthquake- and blast-resistant structures.

2) Experimental and theoretical studies on the inelastic deformability of biaxially loaded beam-columns under monotonic and reversible loadings will allow more realistic design.

3) Optimum bracing-spacing studies on beam-columns are needed to arrive at a more liberal and more realistic bracing requirement.

4) Post-buckling deformability, both after local and lateral-torsional buckling, should be investigated.

5) The effects of the loading path, of elastic unloading of previously yielded fibers and of strain hardening should be studied.

6) The influence of encasement of beam-columns on the lateral-torsional buckling behavior needs to be investigated.

7) Further research topics involve the study of

a) Laterally unbraced and end-restrained beam-columns

b) Beam-columns under large axial load (P/P_y = 0.8 to 0.9)

c) Large-sized beam-columns

d) Beam-columns under dynamically applied end moments

e) Restrained beam-columns subjected to drift, with composite and non-composite restraining beams

f) Beam-columns of A572 steel.

4. CONNECTIONS

Plastic design is based on the ability of moments to redistribute themselves throughout the structure. In order for this redistribution to be completed, the connection is required to transmit the full plastic moment of the weaker member framing into it. For this reason "Simple" framing (AISC Type 2 construction) and "Semi-Rigid" framing (AISC Type 3 construction) are not suitable for plastically designed steel frames. The connections

to be discussed here will therefore be "fully rigid" (AISC Type 1 construction).

A great deal of research has been performed on fully rigid connections to establish design methods which ensure that the members at a joint can indeed develop their full plastic moment and rotation capacity. This research, together with the experimental evidence and the design rules (Refs. 1-2, 4-1, 4-2 and 4-3), has concentrated on the development of design rules for connections so that they would be the stronger link in the joint-member assembly. The actual strength of the connection, as well as its inelastic deformation, was thus not a primary function of the research.

The major research papers on the behavior of connections which are required to permit the members to be connected to develop their full moment capacity are: Ref. 4-4, welded interior beam-to-column connections; Ref. 4-5 through 4-9, welded corner connections; and Refs. 4-10 through 4-13, high-strength bolted moment resistant connections. The analytical studies of these types of connections, supported and supplemented by extensive experimental studies, have provided design rules (see Ref. 4-3 for a convenient tabular summary). These design rules assure that the connections will permit the members framing into them to achieve their full moment and rotation capacity. The evidence in support of this statement is summarized in Ref. 4-14, which presents many available experimental load-deformation curves for fully moment-resistant connections.

It would thus seem that the strength and energy absorbing capacity of a rigid frame, as well as the rotation capacities of each plastic hinge, can be assessed by assuming rigid connections and plastic hinges in the members adjacent to the connections. The frame test reported in Ref. 4-15 has indeed borne this out, and the ultimate loads of these frames were successfully predicted by assuming that plastic hinges formed at a distance equal to the depth of the member away from the face of the welded beam-to-column connection. This is, of course, a gross simplification of the true situation, even though the over all behavior of the rigid frame can be explained by it. Portions of the connection will yield, and the load-deformation behavior of the joint-member assembly shows that the connection is not fully rigid. However, it is rigid enough to permit the beam to develop its full moment capacity. The amount of rotation contributed by the connection, and the energy absorbed by it, has not been assessed theoretically, even though experimental measurements of connection deformation are available [4-4, 4-9]. This contribution to the rotation has, however, not been defined in terms of the total rotation, and it has not been theoretically predicted.

It is, therefore, desirable to perform more research to determine the contribution of the connection itself to the total deformation of the joint so that the energy absorbed by the inelastic deformation in the connection can be determined. The energy absorbed by a connection is probably quite small when compared to the energy absorbed by the wide-flange member which has a plastic hinge that rotates its full amount. However, in a structure subjected to several load reversals, but which never develops a full mechanism as might be the case for a structure in an earthquake, the energy absorbed by the connections may be considerable.

There have been a number of frame tests (e.g. Refs. 2-37, 4-15, 4-16 and others discussed in the subsequent section) which had connections proportioned by the methods proposed for plastically designed frames, and, with the exception of one test, no mention was made of unsatisfactory connection behavior. All of these frames behaved as predicted by plastic analysis, and so it is concluded that the methods of connection design are adequate. A brief paragraph in Ref. 2-37 states that ". . . . observation of the connection behavior in the tests indicate that the effect of axial load on connection design should be studied. Current methods for proportioning connections do not consider the effect of axial load on the yield criterion of the web." Thus there seems to be some question as to the adequacy of beam-to-column connections for columns with relatively high P/P_y ratios. Subsequent reports (Refs. 4-15

and 4-16) on the same research project, and a new research proposed from the same organization [4-17], do not further mention the problem. It would be desirable to examine the current beam-to-column connection design rules (Ref. 4-3) to see if high axial loads in the columns indeed change anything.

There is some experimental evidence that beam-to-column connections do not introduce any additional problems if the joint is subjected to load reversal. In Ref. 4-8, four square knees (square corner connections) were tested so that the knees opened up under tensile loading. The four specimens were previously tested in compression well beyond the peak of the load-deflection curve, and the connections were therefore already distorted by some local and lateral deformations. In Fig. 16 two of the four moment-deflection curves* are shown from Ref. 4-8. The dashed line is the plastic moment of the connected members; curve A is the compression test, and curve B is the tension test. Comparison of the two types of curves shows that in the region below the M_p of the member, the tension knee is less stiff. This is due to the prior local and lateral deformations in the compression test. However, the tensile test had a larger rotation capacity than the prior compression test; M_p of the connected members was exceeded, and the maximum moment either exceeded or was equal to the maximum moment from the compression test. Three of the four tension tests failed by inelastic instability (local and/or lateral deformation of the compressed elements). The fourth test was made on a knee with very large members (36WF230) and failure occurred by tensile brittle fracture after a moment equal to the maximum moment attained by the compression test was reached.

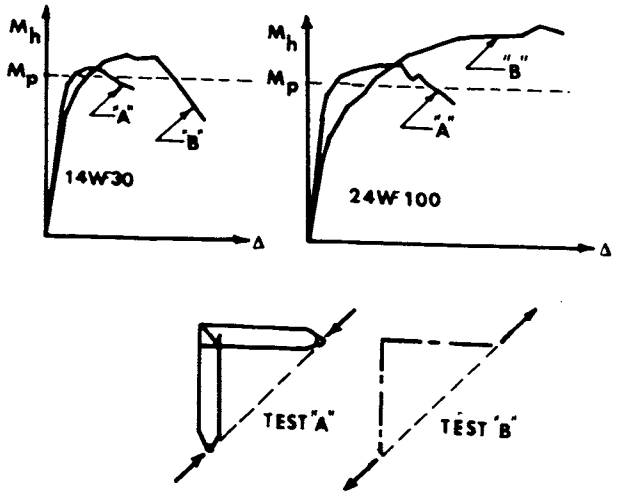

Fig. 16 Connection test results from Ref. 4-8.

* M_h = moment at the intersection of the center lines of the two members

Δ = deflection of the end of the legs relative to each other.

Typical beam-to-column connections were tested under large cycling strains at the University of California at Berkeley [2-45] [2-46]. In these tests cantilever beams were connected to a short column by three typical welded and one typical high-strength bolted beam-to-column connections. The welded connections all failed by alternating plasticity in the beam flange or flange connection plates, and the bolted connection failed by the fracture of the beam-flange across the line of bolts farthest from the column face. In all cases, many cycles at very high strains were delivered by the beam-and-column assembly before failure.

Several steel frames were tested under reversed horizontal loading at Lehigh University (see Refs. 4-16, 4-18 and 4-19). The connections in all these frames were designed by current methods of plastic design (Ref. 4-3), and in every case it was noted that the connections permitted the frame members to develop their full capacity.

The test referred to above seem to indicate that current plastic design methods of connection design are adequate for frames subjected to severe reversed loading. Further testing on various other rigid beam-to-column connections would be highly desirable to determine whether connections which are adequate for monotonic loading are also adequate for reversed loading. Special attention should be paid to connections with columns under high axial load, to connections which consist of two beams framing into a column where one beam is substantially larger than the other [4-14], and to one-sided beam-to-column flange connections.

5. FRAMES

The previous chapters reviewed the status of knowledge on the inelastic rotation capacity of individual beams, beam-columns and connections. They demonstrated that the rotation capacity of beams and beam-columns can be conservatively determined and that connections, if properly designed, will permit the members to develop their full capacity. In order to attain the full available rotation capacity, members must be properly braced against lateral buckling and the width-thickness ratios must not exceed certain specified maximum values.

The review of the inelastic deformability of members gave information on what members can do. This chapter will deal with what members must be able to do in order that the behavior of the frames, of which the members are part, can be satisfactorily predicted. This discussion will be almost entirely restricted to planar frames, that is, the loading will cause deformations primarily in the plane of the frame. Unfortunately, not enough knowledge is available on the inelastic behavior of space frames to make a general review and specific conclusions.

There are two things we might wish to know about a given frame. First, it is desired to know the load-deformation path of the frame under a specified static proportional and monotonic load system (Fig. 17). One point of interest is the relationship of the maximum load to the working load (i.e., the "load factor"), and the other is the force level corresponding to the allowable deflection limit. Such a load-deformation curve is the basis of plastic design, where the load capacity is defined by the maximum load. It is also useful for allowable stress design, where the elastic limit is considered as the limiting load capacity.

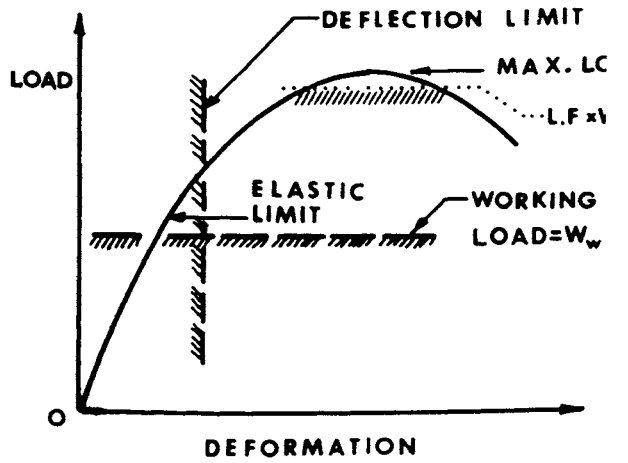

Fig. 17 Load-deformation curve for frame under monotonic proportional loading.

The second item of importance is the energy absorbed by the frame under dynamic, non-proportional and non-monotonic loads. There seems to be no convenient graphic way of representing this information. In fact, the problem still needs to be more clearly defined.

The following discussion examines the literature on both these problems.

Plastic Analysis of Planar Frames

Plastic design requires that the load level corresponding to the working load times a specified load factor be as close as possible but never more than the maximum load which can be supported by the frame (see Fig. 17). The load is assumed to be monotonic, static and proportional; i.e., it increases slowly from zero load, and all loads in the load system remain in a fixed ratio to each other throughout the entire loading history. [1-2] Under these assumptions there exists a unique load-deformation path in the inelastic range. [5-1] The problem of plastic analysis is to estimate this path and to determine the magnitude of the maximum load.

The theoretical determination of the inelastic portion of the load-deformation path for even relatively simple frames is feasible only by making use of the plastic hinge concept. This concept assumes that the moment-rotation curves of the beams and beam-columns are idealized to consist of an elastic portion (linear) up to the plastic moment and of a flat portion where the moment remains unchanged while rotation can continue up to the limiting rotation capacity (see dashed curve in Fig. 1). According to this assumption the whole frame remains elastic except at the point-locations where the moment diagram has extreme points and where plastic hinges form. [1-2]

The first order plastic analysis of a frame proceeds as follows: At first the frame is subjected to small loads so that it is entirely elastic. Frame deflections are not included in the equilibrium equations. The load corresponding to the formation of the first hinge is determined as that load which would cause the highest elastic moment to be equal to the plastic moment. Upon a further increase of load, a real hinge with constant plastic moment is assumed at the first plastic hinge, and the frame has a reduced stiffness in the corresponding elastic analysis. The next hinge forms when the highest moment in this analysis is set equal to M_p. This step-by-step elastic analysis is continued until the stiffness of the frame becomes zero. At this time enough hinges have developed so that the structure with its hinges becomes a mechanism.

This type of an analysis is called "elastic-plastic" analysis, and it gives the best possible first order estimate of the load-deformation path. [5-1] This method is especially convenient with a computer, and a number of fairly complex frames have been analyzed in this manner (see Refs. 2-2, 2-4, 4-15, 4-16, 4-18, 5-2 and 5-3).

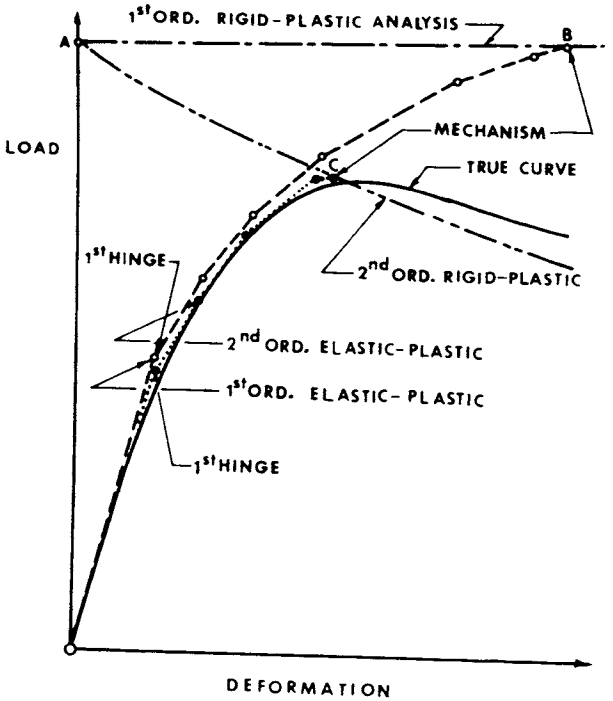

Fig. 18 Types of structural analysis.

For simpler frames, that is, two or three-story, three or four-bay structures, the work involved in the elastic-plastic analysis can be avoided by directly determining the maximum load and the deflections corresponding to the start of mechanism motion, by the rigid-plastic analysis [1-2]. This method becomes, however, rather difficult for more complex frames as it is not possible to account for certain "second-order" effects which become important for complex frames.

The curves in Fig. 18 explain the relationship between various possible types of analysis and the "true" load-deflection curve which might be obtained in an experiment (solid curve). A rigid-plastic analysis will provide the maximum load at point A. If it is assumed that the deformations do not change the force distribution in the frame (that is, first order analysis), the structure will deform as a mechanism without a change in load (line AB). However, if it is assumed that after the start of mechanism motion the internal forces change because of the moments caused by the vertical forces times the deflections ($P - \Delta$ effect), a drooping line, marked "second order rigid-plastic analysis" in Fig. 18 results. As the deformations due to mechanism motion increase, more and more of the moment capacity of the members is taken up by $P - \Delta$ moments and in order to maintain equilibrium the load capacity must be reduced. The curve marked "first order elastic-plastic analysis" is a step-by-step analysis as described before where the $P - \Delta$ moments are ignored. This curve reaches the first order rigid plastic curve at B when the first order maximum load is reached. This is an upper bound to the true maximum load. The second order elastic-plastic analysis is computed by including the $P - \Delta$ effect and it joins with the second order rigid-plastic curve at C. It so happens that on this schematic diagram point C is also the maximum load. This need not necessarily be so, and the intersection may take place after the maximum load is reached. Thus it is possible, and for complex frames quite probable, that the maximum load according to the second order elastic-plastic analysis occurs before a complete mechanism has

formed. [5-3] This is due to the fact that the stability of the frame may deteriorate because of axial forces and plastic hinges before a mechanism occurs.

The maximum point on the second order elastic-plastic load-deformation curve is the best estimate of the true maximum load which can be made for all but the simplest frames. Beyond the peak point of the curve, strain-hardening effects become predominant and an analysis which neglects strain-hardening will generally fall below the "true" curve. [4-15] However, methods are available to deal with this problem also (Ref. 4-15), so that the course of the curve past the peak can be analyzed more realistically.

For many smaller structures, e.g., continuous beams, shed-type frames and low buildings, the second order effects are negligible or easily approximated, and the first order rigid-plastic analysis predicts the total maximum load capacity with very good accuracy. This fact is the basis for the success of plastic design for such structures whose design is governed by Part 2 of the 1963 AISC Specification [1-5]. There is a great deal of experimental evidence of this from tests of continuous beams, square and gabled one-story, two-story, one-bay and two-bay frames made up of full-sized steel members.

This experimental evidence is catalogued in the references cited in Refs. 1-1 and 1-4. In Chap. 5 of Ref. 1-1, out of a total of 18 beam tests and 22 frame tests, only one beam and three frames delivered slightly less than the predicted first order rigid-plastic maximum load. The other structures either exceeded or delivered exactly the predicted loads. Thus for these types of structures where axial loads are relatively small, there is no doubt about the validity of the theory. These tests also showed very good agreement with the complete load-deformation curve as determined by first order elastic-plastic theory.

Relatively high axial forces have three effects on the load-deformation relationship: 1) they introduce additional moments due to the $P - \Delta$ effect; 2) they reduce the elastic stiffness of the beam-columns; and 3) they introduce additional moments due to member shortening. Of these three the $P - \Delta$ effect is the most important. The other two may or may not be significant, depending on the type of loading and geometry.

The reduction in the elastic flexural stiffness of the columns is negligible as long as the following relationship holds [5-3]:

$$L \sqrt{P/EI} < 1.0 \qquad (39)$$

where L is the height of the story, P is the axial load in the column, and EI is its elastic modulus times the moment of inertia. Complete results on the effects of the member shortening are not available, but studies on one and two-bay frames of up to 15 stories have indicated that the reduction of the maximum load due to axial shortening is not significant. [5-3] The closer the frame is to a mechanism at the peak of the load-deflection curve, the less significant is the influence of this effect.

An iterative type second-order elastic-plastic analysis has been developed for taking care of the second-order effects (Refs. 2-2, 2-4, 4-15, 4-16, 5-2 and 5-3). This type of analysis is necessarily a computer solution. A method of plastic design, including the design against second-order effects, but distinctive from the analysis method, has also been developed [5-4]. Thus a theoretical basis exists for both the analysis and the design of steel multistory frames.

The establishment of a broad experimental basis for the verification of the second-order elastic-plastic analysis may be practically quite expensive. It is not feasible to test many full-scale multistory frames, although it is hoped that at some time in the future such a test will be performed on a building to be dismantled.

There is also a possibility of extensive model tests and a good start on such tests has already been made [5-15]. The existing laboratory tests are on full-scale frames of up to three 10-ft.-high stories, and two 15-ft.-wide bays which were performed at Lehigh University. The structural details of one of these tests, reported in Ref. 4-15, are given in Fig. 19. The vertical loads were applied first, and

kept constant as the horizontal load H was applied. The solid curve in Fig. 20 is the experimentally obtained relationship between the horizontal load H and the horizontal deflection at the beam level, Δ. The dashed curves show that the total load-deformation relationship was well predicted by an elastic-plastic analysis up to the maximum load, and by an analysis which included the effect of strain-hardening after that point. The fact that the maximum load predicted by first order rigid plastic theory of 21.3 kips was substantially above the actual maximum load of 16.9 kips shows that the $P - \Delta$ effect was quite considerable for this frame and load system.

Three tests on three-story, two-bay frames braced by diagonal bracing and which were loaded by: 1) symmetric vertical forces, 2) unsymmetric vertical forces, and 3) horizontal and vertical forces, showed good agreement with theoretical predictions as regards the maximum loads, the load-deformation paths and the order of hinge formation. [2-37]

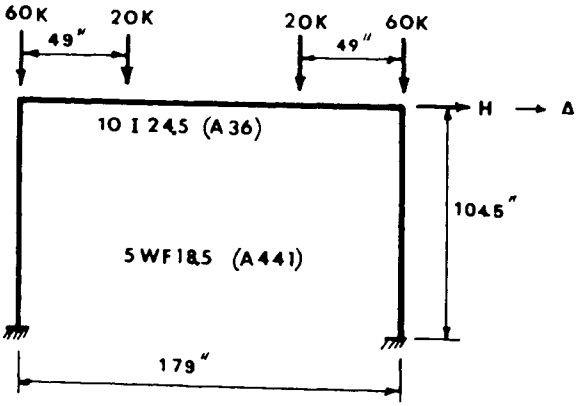

Fig. 19 Test frame of Ref. 4-15.

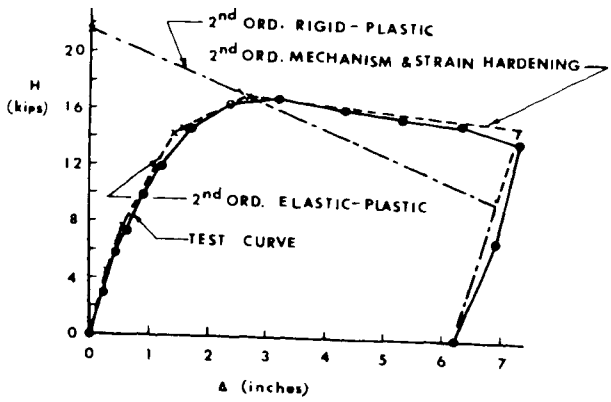

Fig. 20 Comparison of test results with theory for the frame of Fig. 19.

Similarly good correspondence was obtained for tests on two three-story, one-bay and one three-story, two-bay unbraced frames [4-16].

The seven frame tests at Lehigh (Refs. 4-15, 2-37, and 4-16, with the testing technique reported in Ref. 5-5) demonstrate that the behavior of such frames is quite adequately predicted by the second-order elastic-plastic analysis.

The design procedure recommended for the plastic design of multistory frames is not based on an elastic-plastic analysis of the whole frame, but on the design of individual subassemblages consisting of one column member and the beams framing into it. [5-4] A great deal of theoretical work was performed (Refs. 3-4, 3-9, 5-6, 5-7, 5-8, and Chapters 9, 10, and 17 in Ref. 5-4) to develop efficient means of predicting the load-deformation curves for these subassemblages. This theoretical work was verified by a series of tests on columns restrained at their ends by beams. These tests are reported in Refs. 2-18, 3-12, and 5-9, and excellent correlation was obtained between theoretical and experimental moment-rotation curves and maximum loads. These tests are remarkable in that the column members were often deformed well into the descending branch of their end moment-end rotation curves before the whole subassemblage reached its maximum load.

The frame and subassemblage tests provide a substantial and convincing experimental basis for both the plastic analysis as well as the plastic design of planar multistory rigid frames. It should be pointed out that in all of these tests, lateral bracing was used to guard against lateral torsional buckling, and the details of all phases of the testing were carefully controlled and supervised.

Rotation Requirements and Rotation Capacities

The problem of comparing the required hinge rotation at a plastic hinge with the available capacity has not received recent attention. If the load-deformation curve is determined by computer, the required hinge angles are a by-product of the computations and comparison can be made with the rotation

capacity which is available. The available rotation capacity can be obtained from Eqs. 17 or 20 for beams and from Figs. 14 or 15 or from the available $M-\theta$ charts in Ref. 3-10 for beam-columns.

Rotation capacity requirements for structures where the $P-\Delta$ effect is negligible, that is, continuous beams and single-story frames, are studied in Refs. 5-10 and 5-11. Rotation capacity requirements are compared with available rotation capacities in Ref. 2-42 for three-span continuous beams. An examination of the results in these reports leads to the following conclusions:

1) Members under uniform moment usually form hinges late in the deformation history, and the required rotation is considerably less than the capacity.

2) Under common structural situations, it is unlikely that the rotation requirement exceeds the rotation capacity for hinges forming in regions of steep moment gradient. In uncommon situations, for example, for three-span beams with much heavier loads on the end spans than in the center span, and for gabled frames with steep gables, large theoretical rotation requirements may be computed using elastic-plastic theory.

In considering the comparisons between the available and required hinge rotation capacities, it should be realized that the available capacity is based on a strain-hardening model, whereas the required capacity has been computed by neglecting strain-hardening. Strain-hardening alters the moment distribution, it stiffens the beams and it appears to reduce deformations [2-41]. The discussion in Chapter 2 has also shown that the prediction of the available rotation capacity may be quite conservative. It seems desirable to further investigate the required rotation capacity by including strain-hardening for structures of the type considered in Refs. 5-10, 5-11, and 2-42.

No exhaustive studies of these problems have as yet been performed for multistory frames where a second-order elastic-plastic analysis must be performed. However, both Parikh (Ref. 2-4) and Korn (Ref. 5-3) give maximum hinge rotations for the frames they have analyzed. From a knowledge of the material and section properties, and from the final moment diagram, it is possible to compute the available capacity from Eq. 20. The rotation capacity exceeds the requirement for both frames in Ref. 2-4 (10-story, 3-bay, and 24-story, 3-bay frames). The maximum hinge angles at collapse and the computed available rotation capacities are tabulated in Table 7 for the frames which were analyzed by a second-order elastic-plastic analysis in Ref. 5-3. This table shows that in all except four cases the capacity substantially exceeded the requirement. For the four frames where this was not so, the rotations in the parentheses show the maximum hinge angles at a load only slightly below the collapse load. These rotations are substantially smaller than the rotations at collapse, indicating that the particular frames were very ductile in the final stages. However, the rotations still exceed the capacities in three cases. Two of the three frames (four-story, one-bay, and eight-story, one-bay) had extremely flexible beams (weak-beam design) and thus the large rotation requirement is to be expected. The last frame (six-story, two-bay) was subjected to checkerboard loading.

These limited studies on the comparison of the rotation requirement with the rotation capacity seem to indicate that in usual structural situations the capacity exceeds the requirement. However, this is not fully proven, and considerable analytical work is still needed to delineate structural parameters where no additional rotation check needs to be made.

In connection with Table 7 there are several important points worth noting: The hinges with the most rotation usually occur in regions of high moment gradient, that is, at the ends of the beams. For such situations it was demonstrated that the theoretical capacity as defined by Eq. 20 is quite conservative. There is also evidence that the rotations may be smaller if the load-deformation curve is determined by a theory which includes the strain-hardening effect. [2-41]

There are thus quite a number of loose ends in this problem which would warrant further investigation, and thus the results presented in Table 7 should be considered pre-

liminary, and should not be interpreted as having any general validity.

Behavior of Frames Under Reversed Loading

The largest share of the research on frames concerns the maximum strength under static monotonic loading. This type of loading is usually considered to be a satisfactory approach to the design of frames under predominantly static or quasi-static loadings, although there may be a question if this concept will not be challenged as methods of dynamic computer analysis are applied to more complex frames. No structure is subjected to truly static or truly monotonic loads. In a sense the maximum load capacity under static, monotonic and proportional loads is a reference load against which working load levels are compared by means of a minimum allowable load factor. This load factor is really only an empirical parameter which defines past satisfactory behavior. Thus there is still a lack of a truly rational means of defining criteria of design for any structure.

There is, however, one point in favor of the present method of design which is provided by the concept of the shakedown load. A structure will shakedown finally into a fully elastic state if it is possible to find a residual bending moment distribution which, if added to extreme values of elastic bending moments due to the variable repeated loading, will give a resultant moment field which nowhere exceeds the plastic moment (Ref. 1-1, Chap. 6). Methods are available for computing the load level at which shakedown will just take place. This load level is the maximum which can be attained under variable repeated loads. Studies on continuous beams and relatively simple frames have shown that the shakedown load level is only slightly below the maximum load determined by first order rigid-plastic theory. It is argued that the chances of attaining one overload to the static maximum load level are larger than the chances of many severe variable loadings of an intensity only slightly below this level. A design method based on the assumption of static proportional loading is thus justified [1-1].

This argument is justified for the relatively simple structures for which AISC permits plastic design. Besides the analytical evidence, there are also several experiments which bear this out (see the results and references cited in Chap. 6 of Ref. 1-1). The analytical studies, however, are based on structures in which only bending is present. There is a real need to know what happens with regard to the shakedown load when substantial axial loads are present and where such

Table 7. Rotation Requirements and Capacities for Multistory Frames

Type of Frame	Maximum Hinge Angle in Beam (Radians)	Available Rotation Capacity (Radians)
Two-Story, One-Bay	0.0541	0.052
Four-Story, One-Bay	0.0392 (0.0273)	0.020
Eight-Story, One-Bay	0.0357 (0.0297)	0.026
Eight-Story, One-Bay	0.0032	0.023
Eight-Story, One-Bay	0.0049	0.028
Eight-Story, One-Bay	0.0140	0.021
Eight-Story, One-Bay	0.0084	0.021
Eight-Story, One-Bay	0.0207	0.028
Eight-Story, One-Bay	0.0018	0.024
Eight-Story, One-Bay	0.0048	0.024
Eight-Story, One-Bay	0.0077	0.026
Fifteen-Story, One-Bay	0.0303 (0.0223)	0.024
Three-Story, Two-Bay	0.0306	0.035
Six-Story, Two-Bay	0.0171	0.026
Six-Story, Two-Bay	0.0443 (0.0389)	0.026

secondary phenomena as the $P-\Delta$ effect play a predominant role, as for example in steel multistory frames. In the author's opinion, an argument can be made for retaining the concept of design based on proportional loading for many strucutres. This is a current and largely unsupported judgment which may be modified by further research. [5-16]

There are two types of structures where a design based on the maximum proportional load level is incorrect: continuous beam bridges under moving load, and frames which must absorb energy due to earthquake or blast. For beams, one basis of design against severe overload from moving vehicles is the shakedown load. This is always above the elastic limit load, but it may be below the plastic collapse load [5-12]. In the design of frames against severe earthquake or blast shocks, it is desired to absorb energy by inelastic deformation without loss of life by the full destruction of the frame. Thus the attainment or survival of a static load level is not necessarily an adequate criterion. [2-43]

There are essentially two basic approaches available for dealing with the problem of inelastic response to severe dynamic loads. One of these is the "reserve energy" technique (see Ref. 5-13 for a description and for further literature on this subject) which makes empirical use, in part, of static load-deflection curves of the type shown in Fig. 17 for determining energy absorption capacity. This technique is essentially an empirical design method which, while not able to rationally take care of all phenomena involved, appears to be an improvement over the usual quasi-static elastic design. The other approach is to make a dynamic analysis of a given structure for a given excitation and to determine the extent and the number of excursions into the inelastic range. [2-5] [2-43] In this analysis it is necessary to specify a moment-rotation response of each member. A simple elastic-plastic response (Ref. 2-5), and Ramberg-Osgood type relationship (Ref. 2-43) have been used. The criterion of adequacy has as yet not been clearly defined. One criterion would be to determine the extent of inelastic rotation and the number of reversals, and to check these against the rotation capacities of the members. Data on the capacity to resist inelastic load reversals are available from Popov's and Bertero's tests (Refs. 2-44, 2-45, 2-46). Another criterion would be to compare the available energy capacity with the energy which needs to be absorbed. [2-43]

The energy absorption capacity can be very roughly approximated as the sum of the plastic moment times the inelastic rotation at the location of plastic hinges. This information is available for beams and beam-columns under monotonic loading, but such information is still unavailable if the loading is reversed (see previous portions of this report). There is thus need for information about the behavior of individual beams, beam-columns and connections under reversed loading which then can be utilized in making realistic dynamic studies.

Such studies are under way at the University of California at Berkeley (See Ref. 2-5 and 5-17 for the results of such studies), at the California Institute of Technology [5-19] and at the University of Michigan at Ann Arbor [2-43, 5-18]. These studies have been made, to date, without considering the $P-\Delta$ effect, but strain-hardening effects have been included in one of the studies [2-43, 5-18]. This latter effect is incorporated in a Ramberg-Osgood load-deformation diagram, and it seems that both the extent of yielding and the number of reversals were reduced. Strain-hardening is thus beneficial, physically always present, and should therefore be used in an inelastic dynamic analysis. Similar conclusions were also reached by Lay about static proportional loading [2-41].

The $P-\Delta$ effect, though it can result in a considerable reduction in the static proportional maximum load, has also some beneficial effects which make it desirable to include it in future dynamic analyses. One of these is illustrated in Ref. 5-3 where maximum hinge rotations are computed for several frames with the $P-\Delta$ effect included and excluded. The hinge-rotations for the second order analysis were shown to be, for the most part, less than the rotation capacities (Table 7). However, all of these rotations at collapse were higher, some by factors of two or three, for a first order

analysis ($P - \Delta$ effect neglected). Thus the internal behavior of the frame was more reasonable and attainable for the more realistic second-order analysis.

Another effect of the axial forces is illustrated in Fig. 21 which shows the horizontal load-versus-horizontal deflection behavior of the frame in Fig. 19 under the reversal of the load *H* as the vertical loads remained constant. The first branch of the curve is the same as Fig. 20; the other branches result from repeated reversed loading. The most significant aspect of this test is that the maximum loads which could be carried by the frame in all but the first load application are increased substantially. Thus a remarkable increase of capacity exists upon reloading in the opposite direction and upon further cycling after that. This same observation was made also in two other tests where a three-story, one-bay frame, and a three-story, two-bay frame were tested in a similar manner. [4-16] [4-19]

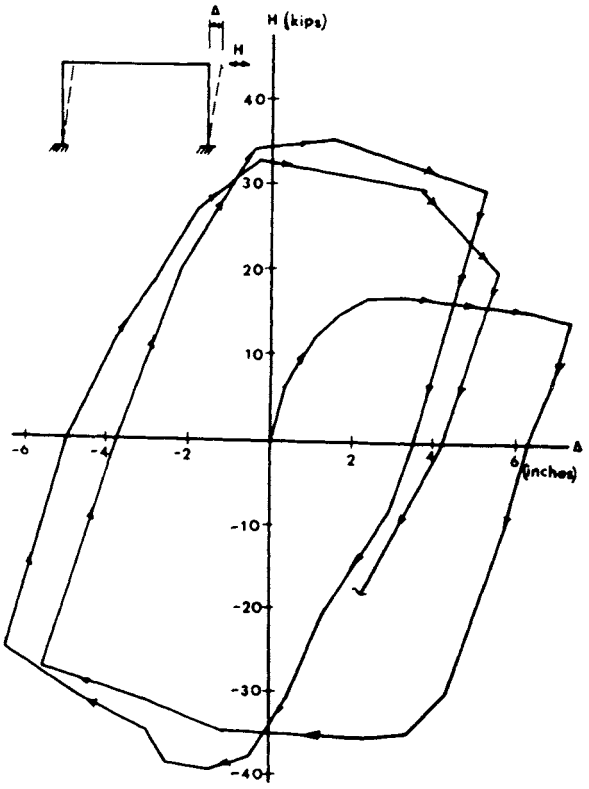

Fig. 21 $H-\Delta$ Curves for hybrid frame.

The maximum loads attained in each half-cycle for each of these three frames is listed in Table 8. It is apparent that the same frame was considerably stronger than its original strength when the load was reversed. In no case had the strength level decreased to the value of the original strength in the last cycles of the test. The increase in strength is quite substantial; this increase is ((39.5 - 16.9)/16.9) 100 = 134% for the hybrid frame, and 41% and 61% for the other two frames, respectively.

These tests establish the fact that a frame behaves differently under reversed loading than under monotonic loading, and that strength is enhanced by load reversal.

The following reasons have been proposed for the strength increase under reversed loading:

1) Strain hardening on successive cycles of load application (Ref. 4-19).

2) Displacement effect; i.e., when the frame deforms the beams drop, and when the load is reversed the vertical loads must be lifted up (Ref. 4-19).

3) After the first one-half cycle, when all horizontal loads are removed from the frame, the residual permanent sway deflections, in conjunction with the remaining vertical loads, create a "residual $P - \Delta$ effect" which must be counteracted by some portion of the reversed loads (Ref. 4-16).

In Ref. 4-18 an attempt is made to incorporate into an analysis both the "residual

Table 8. Maximum Loads of Test-Frames Under Reversed Horizontal Loads

Type of Frame	Maximum Horizontal Load, Kips.				
	½ Cycle	1 Cycle	1½ Cycle	2 Cycle	2½ Cycle
Fig. 19	16.9	36	36	39.5	33
3-Story, 1-Bay	2.9	4.1	—		
3-Story, 2-Bay	5.1	8.2	6.9		

$P - \Delta$ effect" and strain-hardening. In view of the rather simplified assumptions which were made, and due to the uncertainties resulting from a lack of adequate experimental data, it was not possible to describe completely the behavior of the hybrid frame. However, it was shown that a substantial amount of the increase in strength could be accounted for by these effects.

In order to obtain a qualitative idea of the influence of the "residual $P - \Delta$ effect" and strain-hardening, an analysis was performed on the hybrid frame tested at Lehigh [4-18]. The pertinent dimensions of this frame are given in Fig. 22. The vertical loads are all placed only on the column tops (compare with the actual loading of this frame in Fig. 19) in the interests of simplicity. The plastic moment of the beam is considerably higher than the reduced plastic moments of the two columns, and therefore all the inelastic behavior takes place at the column ends where the moments are highest.

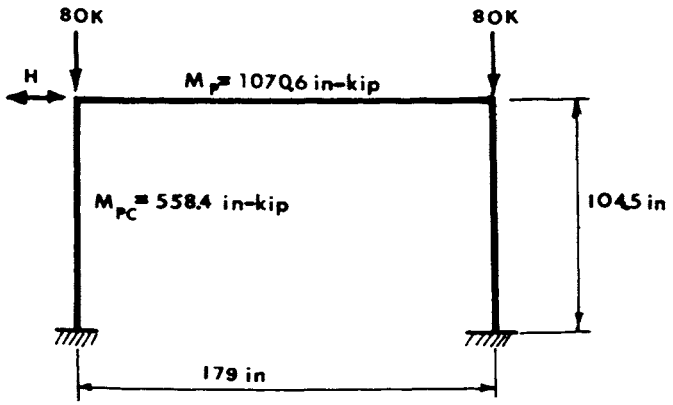

Fig. 22 Simplified frame loading for analytical study.

The moment-end rotation curves used in the analysis are shown in Fig. 23. The top curve is for the case where the effect of strain-hardening is neglected, and the bottom curve includes strain-hardening using the arbitrary stiffness factor J. (Similar relationships were used in Ref. 4-16). In the case of strain-hardening, the elastic range in the unloading branch is always larger than $2M_{pc}$ (Fig. 23b). The Bauschinger effect is completely neglected. This was again done in the interest of simplicity.

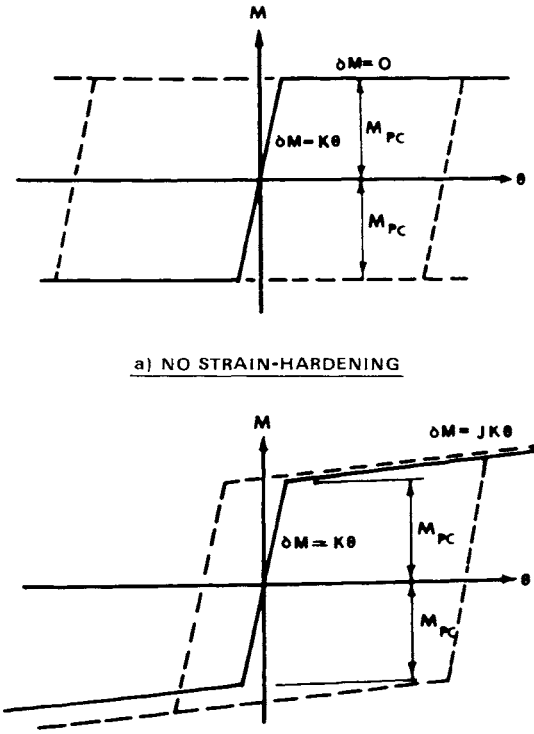

Fig. 23 Moment-rotation relations for columns.

The analysis of the frame was performed by the incremental slope-deflection method discussed in Ref. 4-16. The analysis was performed by ignoring the effects of axial shortening and the stiffness reduction due to axial force. The value of M_{pc} was assumed to be the same in both columns so that the changes in yield condition (i.e. formation of plastic hinges in the case of the elastic-plastic analysis and start of strain-hardening in the case of the elastic-strain-hardening solution) were the same in each column. These latter assumptions were again made in order to achieve a simple solution. However, these effects are small in this frame, and no large error results by making them.

The results of the analysis are given in Fig. 24 for the elastic-plastic analysis, and in Fig. 25 for the elastic-strain-hardening analysis. The curves show the relationship between the horizontal force H and the resulting column rotation ρ.

Elastic-plastic Analysis (Fig. 24)

Curve OABEC represents monotonic loading. At point A plastic hinges form at the

base of the columns, and the full sway mechanism has developed at point B. At an arbitrary rotation $\rho = 0.07$ radians, the horizontal load is released first and then it is reapplied in the opposite direction. Branch EFGHI gives the second part of the loading cycle. It can be seen that the load required to initiate yielding, or to reach the maximum value in the reverse direction, is proportionately higher than the first maximum load (in this case these loads are −27.0 kips and 18.5 kips, respectively). The maximum loads in either direction are bounded by the two parallel lines DBEC and JHGK. The two curves cross the H-axis at the load corresponding to first order rigid-plastic theory and their slope is that of the plastic mechanism curve which includes the $P - \Delta$ effect. The more the frame is deformed past the peak of the curve at the first application of the load, the higher is the force required for a mechanism in the other direction.

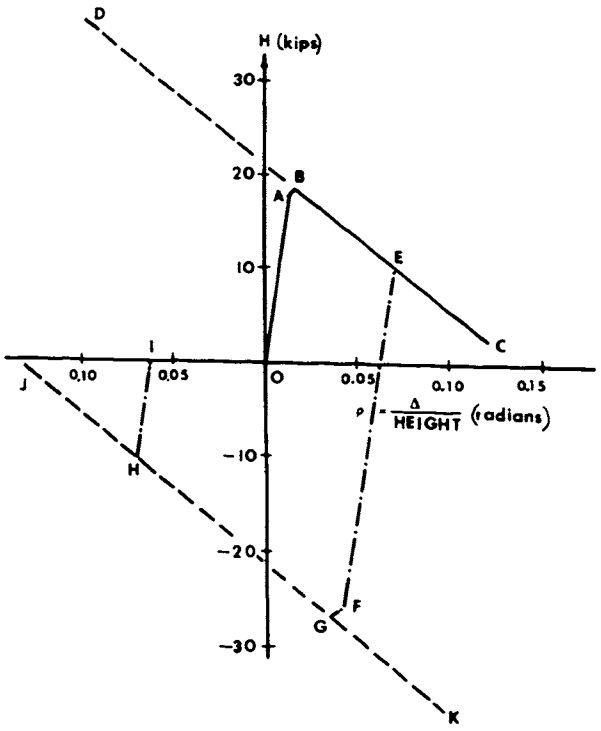

Fig. 24 Frame under load reversal, no strain-hardening.

Elastic-Strain-Hardening Analysis (Fig. 25)

The analysis in Fig. 24 gives only the influence of the "residual $P - \Delta$ effect." The curves in Fig. 25 include this influence plus the effect of strain-hardening. In this particular analysis the strain-hardening stiffness was arbitrarily taken to be 1/10 of the elastic stiffness (i.e., $J = 1/10$ in Fig. 22). The curve OABC represents the first monotonic load application. Strain-hardening does not affect the first maximum load appreciably (18.8 kips versus 18.5 kips in the absence of strain-hardening), a fact which has been noted previously [4-15]. However, the $H - \Delta$ curve is considerably stiffer than the post-mechanism curve in the absence of strain-hardening (compare branch BC with line QP in Fig. 25) after strain-hardening has set in at the bottom and at the top of the columns. Monotonic loading is stopped arbitrarily at $\rho = 0.07$ radians. When the horizontal load is reversed, maximum load is reached at point E, and it is equal to −26.7 kips (as compared with 18.8 kips on the first half cycle). Upon negative straining to −0.07 radians, unloading and reloading again (EFGH) a new maximum of 25.7 kips is reached. If now the frame is strained to $\rho = 0.12$ radians (point I) and then reloaded in the opposite sense (IJKL), the maximum load is −32.6 kips. The model thus shows that if both the "residual $P - \Delta$ effect" and strain-hardening are present, it is possible to

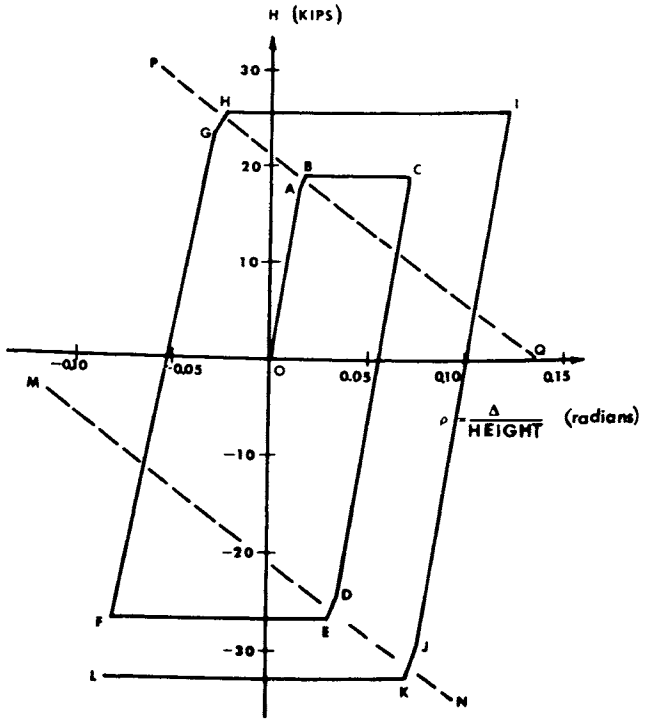

Fig. 25 Frame under load reversal, strain-hardening, $J = \frac{1}{10}$.

increase the strength of the frame. The more the frame is deformed in one direction, the more force is required to obtain maximum load in the other direction.

The few available frame tests under reversed horizontal loading and the very approximate analysis strongly suggest that dynamic analyses of inelastic frames should incorporate the $P - \Delta$ effects and strain-hardening. [5-14] There is also no need to limit inelastic deformations to beams only, since the behavior of columns in the inelastic range can also be included in an analysis.

Research Needs

A rational study of the behavior of complex frames, whether the analysis is based on static or dynamic loads, on elastic or elastic-plastic response, or on first or second order analysis, has become possible only as a result of large digital computers. Such computers became generally available only at the beginning of this decade, and yet it is amazing to note the large variety of problems which have been studied. Structural problems of all types and of any magnitude can be solved in the future, provided that the basic conditions of the solution can be mathematically formulated. It is important that the basic conditions be well understood. In both the static and the dynamic studies the basic conditions of frame analysis are the member load-deformation relationships. The research needs for these have been listed previously. Computer studies of frames should be channeled along the following broad research needs:

1) Analysis methods should be refined to permit efficient static or dynamic analyses of large size plane frames with provisions to include the effects of plasticity, strain-hardening, $P - \Delta$ moments and axial shortening.

2) Parameter studies should be made to determine for what frame geometry and load configurations some or all of the second order effects are negligible, and where they must be included in order to arrive at a realistic interpretation of frame behavior.

3) Static and dynamic analyses on a wide range of frames should be performed to obtain the requirements for inelastic rotation.

4) Careful analytic and experimental studies should be performed on the basis of energy requirements and capacities to permit a consistent and rational definition of the energy absorption capacity of complex frames.

5) The role of non-structural cladding on both the static load-deformation response and the dynamic energy absorption capacity needs to be closely examined both analytically and by experiment.

6) Work on the elastic-plastic analysis of three-dimensional frameworks should be initiated; the questions to be asked need to be formulated clearly before extensive studies are performed.

6. SUMMARY AND CONCLUSIONS

This report has attempted to summarize the status of knowledge on the inelastic deformability of steel members and frames. It was demonstrated in the report that the planar inelastic response of beams, beam-columns and frames is well understood and can be adequately, though conservatively, predicted by theory, provided: 1) the loading is static, monotonic, and proportional and 2) adequate provisions exist to inhibit local and lateral deformations. A great deal of experimental work was performed, and it substantiates the theoretical predictions. The inelastic deformability for members and connections is finally curbed by the combined occurrence of local and lateral deformations at average strain levels of 10 to 15 times the yield strain (i.e. strain-hardening strains). It was shown that the inelastic rotation capacity, which defines both the "ductility factor" and the inelastic energy absorption capacity, is predictable and large enough to meet the rotation requirements of plastically designed frames. Thus the plastic design of steel frames, whether relatively simple or quite complex and large, is based on an adequate and impressive body of knowledge and experimental experience.

The knowledge of the behavior of members and frames subjected to loading which is non-proportional or reversible and which may be a result of dynamic phenomena is less developed. The methods of frame analysis are

available, but information on the behavior of individual structural components under reversed loading into the inelastic range is incomplete. There is not as extensive an experimental basis for such loading as there is for monotonic loading. Such information must be developed before the analysis methods can be considered fully reliable.

There is not enough known about the inelastic behavior of structural steel members which are subject to biaxial loading. Such information must be developed before reliable analysis methods can be formulated.

There are thus two major areas of research which are recommended. These are:

1) Analytical and experimental studies on beams, beam-columns, connections, subassemblages, and small frames, under reversible static and dynamic loading which produces inelastic strains.

2) Tests and theory on the behavior of frames, members and connections under biaxial loading.

Present research is being performed at various institutions on some phases of these areas. However, the problems introduced by load reversal, by strain-rate effects, by biaxial effects, etc., are complex, and therefore it is necessary that the present volume of research be increased to develop the needed body of information for a rational seismic design method.

The large amount of research performed for the development of plastic design has relevance for the study of the behavior of structures subjected to earthquake motion or blast, but it is only a stepping stone which can not provide all the answers.

Research needs on specific topics have been discussed in various parts of the report, and they are tabulated at the end of each chapter.

7. REFERENCES

Chapter 1

1-1 WRC-ASCE Joint Committee
"Commentary on Plastic Design in Steel"
ASCE Manual No. 41, 1961

1-2 L. S. Beedle
"Plastic Design of Steel Frames"
Wiley, New York, 1958

1-3 J. F. Baker, M. R. Horne, J. Heyman
"The Steel Skeleton, Vol. II"
Cambridge University Press, 1956

1-4 M. G. Lay
"The Experimental Bases for Plastic Design"
WRC Bulletin No. 99, Sept. 1964

1-5 AISC
"Specification for the Design, Fabrication and Erection of Structural Steel for Buildings"
AISC, New York, 1963

Chapter 2

2-1 T. V. Galambos
"Beams", Chap. 3 in "Plastic Design of Multi-Story Frames", Fritz Engineering Laboratory Report No. 273.20, Summer 1965

2-2 M. R. Horne, K. I. Majid
"Elastic-Plastic Analysis of Rigid Jointed Sway Frames by Computer"
Research Report No. 1, University of Manchester, Department of Civil Engineering.

2-3 J. H. Daniels
"Examples of Unbraced Frame Design", Chap. 19 in "Plastic Design of Multi-Story Frames", Fritz Engineering Laboratory Report No. 273.20, Summer 1965.

2-4 B. P. Parikh
"Elastic-Plastic Analysis and Design of Unbraced Multi-Story Frames"
Ph.D. Dissertation, Lehigh University, June 1966.

2-5 R. W. Clough, K. L. Benuska, E. L. Wilson
"Inelastic Earthquake Response of Tall Buildings"
Proceedings of the Third World Conference on Earthquake Engineering, Wellington, New Zealand, 1964.

2-6 G. C. Lee
"A Survey of the Literature on the Lateral Instability of Beams"
WRC Bulletin No. 63, Aug. 1963

2-7 R. L. Ketter, E. L. Kaminsky, L. S. Beedle
"Plastic Deformations of Wide-Flange Beam-Columns"
ASCE Transactions, Vol. 120, p. 1028, 1955.

2-8 L. Tall
"Compression Members", Chap. 9 in "Structural Steel Design"
Ronald Press, New York, 1964.

2-9 R. L. Ketter, T. V. Galambos
"Columns Under Combined Bending and Thrust"
ASCE Transactions, Vol. 126 (I) p. 1, 1961.

2-10 A. P. Hrennikoff
"Importance of Strain-Hardening in Plastic Design"
ASCE Proceedings, Vol. 91, ST 4, Aug. 1965.

2-11 P. F. Adams, T. V. Galambos
"Discussion of Ref. 2-10"
ASCE Proceedings, Vol. 92, ST 2, April 1966.

2-12 P. F. Adams, M. G. Lay, T. V. Galambos
"Experiments on High-Strength Steel Members"
WRC Bulletin No. 110, Nov. 1965.

2-13 G. C. Lee, T. V Galambos
"Post-Buckling Strength of Wide-Flange Beams"
ASCE Proceedings, Vol. 88, EM-1, Feb. 1962.

2-14 J. Prasad, T. V. Galambos
"The Influence of Adjacent Spans on the Rotation Capacity of Beams", Fritz Engineering Laboratory Report No. 205H.12, Lehigh University, June 1963.

2-15 G. C. Lee, A. T. Ferrara, T. V. Galambos
"Experiments on Wide-Flange Beams"
WRC Bulletin No. 99, Sept. 1964.

2-16 H. A. Sawyer
"Post-Elastic Behavior of Wide-Flange Steel Beams"
ASCE Proceedings, Vol. 87, ST 8, Dec. 1961.

2-17 M. G. Lay, N. Gimsing
"Experimental Studies of the Moment-Thrust-Curvature Relationship"
Welding Journal Research Supplement, Vol. 44, Feb. 1965.

2-18 P. F. Adams
"Plastic Design in High Strength Steel"
Ph.D. Dissertation, Lehigh University, June 1966.

2-19 G. C. Lee
"Inelastic Lateral Instability of Beams and

Their Bracing Requirements"
Ph.D. Dissertation, Lehigh University, 1960.

2-20 T. Kusuda, R. Sarubbi, B. Thurlimann
"The Spacing of Lateral Bracing in Plastic Design"
Fritz Engineering Laboratory Report No. 205E.11, Lehigh University, 1960.

2-21 ASCE Subcommittee Report on
"Hybrid Steel Beams", Chairman C. G. Schilling
Currently under review for publication in the Structural Journal of the ASCE.

2-22 G. Haaijer
"Plate Buckling in the Strain-Hardening Range"
ASCE Proceedings, Vol. 83, EM2, April 1957.

2-23 G. Haaijer, B. Thurlimann
"Inelastic Buckling in Steel"
ASCE Transactions, Vol. 125, 1960.

2-24 B. Thurlimann
"New Aspects Concerning the Inelastic Instability of Steel Structures"
ASCE Proceedings, Vol. 86, ST-1, Jan. 1960.

2-25 J. F. Baker
"Plastic Design in Steel to BS968"
BCSA Publication No. 21, 1963.

2-26 N. Burnett, L. G. Johnson, L. J. Morris, A. L. Randall, C. P. Thompson
"Plastic Design"
BCSA Publication No. 28, 1965.

2-27 R. Anslijn, E. Mas, C. Massonnet
"The Extension of Plastic Theory of Design to Steel A52"
Preliminary Publication, 7th Congress, IABSE, Rio de Janeiro, Aug. 1964.

2-28 M. G. Lay
"Flange Local Buckling in Wide-Flange Shapes"
ASCE Proceedings, Vol. 91, ST6, Dec. 1965.

2-29 M. G. Lay
"The Static Load Deformation Behavior of Planar Steel Structures"
Ph.D. Dissertation, Lehigh University, 1964.

2-30 M. W. White
"The Lateral-Torsional Buckling of Yielded Structural Steel Members"
Ph.D. Dissertation, Lehigh University, 1956.

2-31 M. G. Lay
"Yielding of Uniformly Loaded Steel Members"
ASCE Proceedings, Vol. 91, ST6, Dec. 1965.

2-32 M. G. Lay, T. V. Galambos
"Inelastic Steel Beams Under Uniform Moment"
ASCE Proceedings, Vol. 91, ST6, Dec. 1965.

2-33 M. G. Lay, T. V. Galambos
"Inelastic Beams Under Moment Gradient"
ASCE Proceedings, Vol. 93, ST1, Feb. 1967.

2-34 M. G. Lay, T. V. Galambos
"Bracing Requirements for Inelastic Steel Beams"
ASCE Proceedings, Vol. 92, ST2, April 1966.

2-35 B. Rawlings
"Energy Relationships in Plastic Steel Structures"
ASCE Proceedings, Vol. 88, ST4, Aug. 1962.

2-36 C. Massey
"Lateral Bracing Forces in Steel I-Beams"
ASCE Proceedings, Vol. 88, EM6, Dec. 1962.

2-37 J. A. Yura
"The Strength of Braced Multi-Story Steel Frames"
Ph.D. Dissertation, Lehigh University, June 1966.

2-38 M. G. Lay
"The Deformation Capacity of Stocky Steel Members"
Trans. Inst. Engineers of Australia, CE6(2), Oct. 1965.

2-39 G. C. Driscoll, Jr., L. S. Beedle
"The Plastic Behavior of Structural Members and Frames"
Welding Journal, 36 (6), June 1957.

2-40 E. Popov, J. Willis
"Plastic Design of Cover-Plated Continuous Beams"
ASCE Proceedings, Vol. 84, EMI, Jan. 1958.

2-41 M. G. Lay
"A New Approach to Inelastic Structural Design"
Proc. Instu. of Civil Engineers, Vol. 34, May 1966.

2-42 R. P. Kerfoot
"Rotation Capacity of Beams"
Fritz Engineering Laboratory Report No. 297.14, Lehigh University, March 1965.

2-43 G. V. Berg
"A Study of the Earthquake Response of Inelastic Systems"
Preliminary Reports – Earthquake Response of Steel Frames, AISI, Feb. 1966.

2-44 V. V. Bertero, E. P. Popov
"Effect of Large Alternating Strains on Steel Beams"
ASCE Proceedings, Vol. 91, ST1, Feb. 1965.

2-45 E. P. Popov and H. A. Franklin
"Steel Beam-to-Column Connections Subjected to Cyclically Reversed Loading"
Preliminary Reports – Earthquake Response of Steel Frames, AISI, Feb. 1966.

2-46 E. P. Popov
"Low Cycle Fatigue of Steel Beam-to-Column Connections"
International Symposium on the Effects of Repeated Loading on Materials and Structural Elements; Mexico City, Sept. 15-17, 1966.

2-47 K. T. Kavanagh
"Blast Resistance of Elastic and Elasto-Plastic Frames"
M.S. Thesis, Cornell University, 1965.

2-48 J. D. Morrow
"Cyclic Plastic Strain Energy and Fatigue of Metals"
Special Technical Publication No. 378, ASTM, 1965.

2-49 R. D. Hanson
"Post-Elastic Dynamic Response of Mild Steel Structures"
Ph.D. Dissertation, California Institute of Technology, 1965.

2-50 R. D. Hanson
"Comparison of Static and Dynamic Hysteresis Curves"
ASCE Proceedings, Vol. 92, No. EM5, Oct. 1965.

2-51 P. P. Benham
"Fatigue of Metals Caused By Relatively Few Cycles of High Load as Strain Amplitude"
Metallurgical Reviews, Vol. 3, No. 11, p. 203, 1958.

2-52 D. S. Dugdale
"Stress-Strain Cycles of Large Amplitude"
Journal of Mechanics and Physics of Solids, Vol. 7, No. 2, p. 135.

2-53 P. P. Benham
"Low Endurance Fatigue of a Mild Steel and an Aluminum Alloy" Journal of Mechanical Engineering Science, 3, No. 2, June 1961.

2-54 L. F. Coffin, J. E. Tavernelli
"The Cyclic Straining and Fatigue of Metals"
Met. Soc. AMIE Trans. 215, p. 794, Oct. 1959.

2-55 R. Royles
"Fatigue of Ductile Structures in Reversed Bending"
Ph.D. Thesis, Cambridge University, England. 1964.

2-56 S. Krishnasamy, A. N. Sherbourne
"Mild Steel Structures Under Reversed Bending"
International Symposium on the Effects of Repeated Loading on Materials and Structural Elements, Mexico City, Sept. 15-17, 1966.

2-57 A. F. Luke, P. F. Adams
"Rotation Capacity of Wide-Flange Beams Under Moment Gradient" Report No. 1, Behavior of High Strength Steel Members, Department of Civil Engineering, University of Alberta.

Chapter 3

3-1 WRC-ASCE Joint Committee
"Commentary on Plastic Design in Steel", Chap. 7, "Compression Members"
ASCE Manual No. 41, 1961.

3-2 L. W. Lu
"Columns", Chap. 4 in "Plastic Design of Multi-Story Frames"
Fritz Engineering Laboratory Report No. 273.20, Summer 1965.

3-3 T. V. Galambos and R. L. Ketter
"Columns Under Combined Bending and Thrust"
ASCE Transactions, Vol. 126, Part I, p. 1, 1961.

3-4 M. Ojalvo
"Restrained Columns"
ASCE Proceedings, Vol. 86, EM 5, Oct. 1960.

3-5 T. V. Galambos
"Combined Bending and Compression" in "Structural Steel Design" ed. L. Tall
Ronald Press Co., New York, 1964.

3-6 M. G. Lay
"The Mechanics of Column Deflection Curves"
Fritz Engineering Laboratory Report No. 278.12, June 1964.

3-7 T. V. Galambos
"Column Deflection Curves" Chap. 9 in "Plastic Design of Multi-Story Frames"
Fritz Engineering Laboratory Report No. 273.20, Summer 1965.

3-8 T. V. Galambos, J. Prasad
"Ultimate Strength Tables for Beam-Columns"
WRC Bulletin No. 78, 1962.

3-9 M. Ojalvo and Y. Fukumoto
"Nomographs for the Solution of Beam-Column Problems"
WRC Bulletin No. 78, 1962.

3-10 B. P. Parikh, J. H. Daniels, L. W. Lu
"Design Aids Booklet"
Fritz Engineering Laboratory Report No. 273.24, Summer 1965.

3-11 R. C. Van Kuren, T. V. Galambos
"Beam-Column Experiments"
ASCE Proceedings, Vol. 90, ST2, April 1964.

3-12 M. G. Lay, T. V. Galambos
"Experimental Behavior of Restrained Columns"
WRC Bulletin No. 110, Nov. 1965.

3-13 T. J. Dwyer, T. V. Galambos
"Plastic Behavior of Tubular Beam-Columns"
ASCE Proceedings, Vol. 91, ST4, Aug. 1965.

3-14 G. Augusti
"Experimental Rotation Capacity of Steel Beam-Columns"
ASCE Proceedings, Vol. 90, ST6, Dec. 1964.

3-15 M. G. Lay, T. V. Galambos
"End-Moment End-Rotation Characteristics for Beam-Columns"
Fritz Engineering Laboratory Report No. 205A-35, May 1962.

3-16 Y. Fukumoto, T. V. Galambos
"Inelastic Lateral-Torsional Buckling of Beam-Columns"
ASCE Proceedings, Vol. 92, ST2, April 1966.

3-17 R. A. Aglietti, M. G. Lay, T. V. Galambos
"Tests on A36 and A441 Steel Beam-Columns"
Fritz Laboratory Report No. 278.14, June 1964.

3-18 T. V. Galambos, P. F. Adams, Y. Fukumoto
"Further Studies on the Lateral-Torsional Buckling of Steel Beam-Columns"
WRC Bulletin No. 115, July 1966.

3-19 C. E. Massonnet
"Stability Considerations in the Design of Steel Columns"
ASCE Transactions, Vol. 127, p. 525, Part II, 1962.

3-20 C. Miranda, M. Ojalvo
"Inelastic Lateral-Torsional Buckling of Beam-Columns"
ASCE Proceedings, Vol. 91, EMG, Dec. 1965.

3-21 B. G. Johnston
"The Column Research Council Guide to Design Criteria for Metal Compression Members"
John Wiley and Sons, N.Y. 1966.

3-22 R. L. Ketter
"Further Studies on the Strength of Beam-Columns"
ASCE Proceedings, Vol. 87, ST6, Dec. 1961.

3-23 A. Ostapenko
"Design of Braced Frames – Beams" Chap. 8 in "Plastic Design of Multi-Story Frames"
Fritz Engineering Laboratory Report No. 273.20, Summer 1965.

3-24 H. Kamalvand, L. W. Lu
"Ultimate Strength of Laterally Loaded Columns"
Fritz Engineering Laboratory Report No. 273.52, Nov. 1966.

3-25 C. Birnstiel, J. Michalos
"Ultimate Load of H-Columns Under Biaxial Bending"
ASCE Proceedings, Vol. 89, ST2, April 1963.

3-26 C. Birnstiel, K. C. Leu, J. A. Tesoro, R. L. Tomasetti
"Experiments on H-Columns Under Biaxial Bending"
New York University School of Engineering and Science, Jan. 1967.

Chapter 4

4-1 WRC-ASCE Joint Committee
"Commentary on Plastic Design in Steel", Chap. 8, "Connections"
ASCE Manual No. 41, 1961.

4-2 J. W. Fisher
"Welded Connections" Chap. 19 in "Structural Steel Design" ed. L. Tall
Ronald Press Co., New York, 1964.

4-3 J. W. Fisher
"Design of Connections" Chap. 5 in "Plastic Design of Multi-Story Frames"
Fritz Engineering Laboratory Report No. 273.20, Summer 1965.

4-4 J. D. Graham, A. N. Sherbourne, R. N. Khabbaz, C. D. Jensen
"Welded Interior Beam-to-Column Connections"
WRC Bulletin No. 63, Aug. 1960 (the same paper is also reprinted as an AISC publication, dated 1959).

4-5 A. A. Toprac, L. S. Beedle
"Further Studies of Welded Corner Connections"
Welding Journal Research Supplement, July 1955.

4-6 J. W. Fisher, G. C. Driscoll, Jr., F. W. Schutz, Jr.
"Behavior of Welded Corner Connections"
Welding Journal Research Supplement, May 1958.

4-7 J. W. Fisher, G. C. Driscoll, Jr., L. S. Beedle
"Plastic Analysis and Design of Square Rigid Frame Knees"
WRC Bulletin No. 39, 1958.

4-8 J. W. Fisher, G. C. Driscoll, Jr.
"Corner Connections Loaded in Tension"
Welding Journal Research Supplement, Nov. 1959.

4-9 J. W. Fisher, G. C. Lee, J. A. Yura, G. C. Driscoll, Jr.

"Plastic Analysis and Tests of Haunched Corner Connections"
WRC Bulletin No. 91, Oct. 1963.

4-10 F. W. Schutz, Jr.
"Strength of Moment Connections Using High Tensile Strength Bolts"
Proceedings, AISC, 1959.

4-11 L. G. Johnson, J. C. Cannon, L. A. Spooner
"High-Tensile Preloaded Joints"
British Welding Journal, Sept. 1960.

4-12 R. T. Douty, W. McGuire
"Research on Bolted Moment Connections"
Proceedings, AISC, 1963.

4-13 R. T. Douty, W. McGuire
"High Strength Bolted Moment Connections"
ASCE Proceedings, Vol. 91, ST2, April 1965.

4-14 L. S. Beedle, R. J. Christopher
"Tests of Steel Moment Connections"
Proceedings of 30th Annual Convention of SEAC, Yosemite, Calif., Oct. 3-5, 1963.

4-15 P. Arnold, P. F. Adams, L. W. Lu
"Experimental and Analytical Behavior of a Hybrid Frame"
Fritz Engineering Laboratory Report No. 297.18, May 1966.

4-16 E. Yarimici
"Incremental Inelastic Analysis of Framed Structures and Some Experimental Verifications"
Ph.D. Dissertation, Lehigh University, June 1966.

4-17 L. D. Carpenter, L. W. Lu, G. C. Driscoll, Jr.
"Proposal for an Exploratory Study on Steel Frames Subjected to Cyclic Lateral Loads"
Fritz Engineering Laboratory Report No. 332.1, Sept. 1966.

4-18 P. Arnold, P. F. Adams, L. W. Lu
"The Effect of Instability on the Cyclic Behavior of a Frame"
International Symposium on the Effects of Repeated Loading on Materials and Structural Elements, Mexico City, Sept. 15-17, 1966.

4-19 L. S. Beedle
"Reversed Loading of Steel Frames – Preliminary Tests"
Preliminary Reports – Earthquake Response of Steel Frames
AISI, Feb. 1966.

Chapter 5

5-1 A. Ostapenko
"Behavior of Unbraced Frames", Chap. 13 in "Plastic Design of Multi-Story Frames"
Fritz Engineering Laboratory Report No. 273.20, Summer 1965.

5-2 M. R. Horne, W. Merchant
"The Stability of Frames"
Pergamon Press, Oxford, England, 1965.

5-3 A. Korn
"The Elastic-Plastic Behavior of Multi-Story, Unbraced Planar Frames"
D.Sc. Dissertation, Washington University, 1967.

5-4 G. C. Driscoll, Jr., et al.
"Plastic Design of Multi-Story Frames"
Fritz Engineering Laboratory Report No. 273.20, Summer 1965.

5-5 E. Yarimici, J. A. Yura, L. W. Lu
"Techniques for Testing Structures Permitted to Sway"
Fritz Engineering Laboratory Report No. 273.40, May 1966.

5-6 V. Levi, G. C. Driscoll, Jr., L. W. Lu
"Structural Subassemblages Prevented From Sway"
ASCE Proceedings, Vol. 91, STS, Oct. 1965.

5-7 V. Levi
"Plastic Design of Braced Multi-Story Frames"
Ph.D. Dissertation, Lehigh University, 1962.

5-8 V. Levi, G. C. Driscoll, Jr., L. W. Lu
"Analysis of Beam-and-Column Subassemblages in Planar Multi-Story Frames"
Fritz Engineering Laboratory Report No. 273.11, 1964.

5-9 M. G. Lay, R. A. Aglietti, T. V. Galambos
"Testing Techniques for Restrained Beam-Columns"
Experimental Mechanics, Vol. 6, No. 1, Jan. 1966.

5-10 G. C. Driscoll, Jr.
"Rotation Capacity Requirements for Beams and Frames of Structural Steel"
Ph.D. Dissertation, Lehigh University, 1958.

5-11 G. C. Driscoll, Jr.
"Rotation Capacity Requirements for Simple Span Frames"
Fritz Engineering Laboratory Report No. 268.5, Sept. 1958.

5-12 A.F.M.R.A. Ghani
"Shakedown Analysis of Non-Prismatic Beams"
D.Sc. Dissertation, Washington University, St. Louis, 1966.

5-13 J. A. Blume, N. M. Newmark, L. H. Corning
"Design of Multi-Story Reinforced Concrete Buildings for Earthquake Motions"
Portland Cement Association, 1961.

5-14 S. Igarashi, N. Taga, S. Takada, Y. Koyanagi
"Plastic Behavior of Steel Frames Under Cyclic Loading".
Transactions A.I.J., Dec. 1966 (Japan).

5-15 W. A. Litle
"Small Scale Models for Steel Frameworks"
AISC Engineering Journal, Vol. 3, No. 3, July 1966.

5-16 J. M. Davies
"Collapse and Shakedown Loads of Plane Frames"
Journal of the Structural Division, ASCE, St. 3, Vol. 93, June 1967.

5-17 R. W. Clough and K. L. Benuska
"Non-Linear Earthquake Behavior of Tall Buildings"
Journal of the Engineering Mechanics Division, ASCE, EM3, Vol. 93, June 1967.

5-18 S. C. Goel and G. V. Berg
"Inelastic Earthquake Response of Tall Steel Frames", Conference Preprint 503, ASCE Structural Engineering Conference, Seattle, Washington, May 8 to 12, 1967.

5-19 P. C. Jennings
"Force-Deflection Relationships From Dynamic Tests"
Journal of the Engineering Mechanics Division, ASCE, EM2, Vol. 93, April 1967.

BULLETINS

Steel Research for Construction

No. 1 Current Paving Practices on Orthotropic Bridge Decks
Battelle Memorial Institute, October, 1965

No. 2 Strength of Three New Types of Composite Beams
A. A. Toprac, October, 1965

No. 3 Research on and Paving Practices for Wearing Surfaces on Orthotropic Steel Bridge Decks
Battelle Memorial Institute, August, 1966

No. 4 Protection of Steel Storage Tanks and Pipe Underground
Battelle Memorial Institute, May, 1967

No. 5 Fatigue Strength of Shear Connectors
R. G. Slutter and J. W. Fisher, October, 1967

No. 6 Paving Practices for Wearing Surfaces on Orthotropic Steel Bridge Decks
Battelle Memorial Institute, January, 1968

No. 7 Report on Investigations of Orthotropic Plate Bridges
D. Allan Firmage

No. 8 Deformation and Energy Absorption Capacity of Steel Structures in the Inelastic Range
Theodore V. Galambos

Committee of Structural Steel Producers • Committee of Steel Plate Producers

american iron and steel institute

150 East 42nd Street, New York, N.Y. 10017